

1 Tectonothermal evolution in the core of an arcuate fold and 2 thrust belt: the southeastern sector of the Cantabrian Zone 3 (Variscan belt, NW Spain)

4 M. L. Valín, S. García-López, C. Brime, F. Bastida and J. Aller

5 Departamento de Geología, Universidad de Oviedo, 33005 Oviedo, Spain

6 *Correspondence to:* Fernando Bastida (bastida@geol.uniovi.es)

7 **Abstract.** The tectonothermal evolution of an area located in the core of the Ibero-Armorican arc (Variscan belt)
8 has been determined by using the conodont color alteration index (CAI), Kübler index of illite (KI), the Árkai
9 index of chlorite (AI), and the analysis of clay minerals and rock cleavage. The area is part of the Cantabrian
10 Zone (CZ), which represents the foreland fold and thrust belt of the orogen. It has been thrust by several large
11 units of the CZ, what resulted in the generation of a large amount of synorogenic Carboniferous sediments. CAI,
12 KI and AI values show an irregular distribution of metamorphic grade, independent of stratigraphic position.
13 Two tectonothermal events have been distinguished in the area. The first one, poorly defined, is mainly located
14 in the northern part. It gave rise to very low-grade metamorphism in some areas and it was associated with a
15 deformation event that resulted in the emplacement of the last large thrust unit and development of upright folds
16 and associated cleavage (S_1). The second tectonothermal event gave rise to low-grade metamorphism and
17 cleavage (S_2) crosscutting earlier upright folds in the central, western and southern parts of the study area. The
18 event continued with the intrusion of small igneous rock bodies, which gave rise to contact metamorphism and
19 hydrothermal alteration. This event was linked to an extensional episode due to a gravitational instability at the
20 end of the Variscan deformation. This tectonothermal evolution occurred during the Gzhelian-Sakmarian.
21 Subsequently, several hydrothermal episodes took place and local crenulation cleavage developed during the
22 Alpine deformation.

23 1 Introduction

24 The Variscan belt defines an arc in the northwestern Iberian Peninsula (Ibero-Armorican Arc), whose core is
25 formed by the Cantabrian Zone (CZ), which represents the foreland fold and thrust belt of the orogen (Fig. 1).
26 This zone consists of Palaeozoic rocks in which two tectonostratigraphic units have been distinguished (Julivert,
27 1978; Marcos and Pulgar, 1982), whose limit is approximately located by the Devonian-Carboniferous
28 boundary. The preorogenic unit is formed of Cambrian to Devonian rocks consisting of alternating carbonate and
29 siliciclastic formations; they form a wedge that thins towards the foreland. The synorogenic unit is formed by
30 several clastic units, also thinning towards the foreland, which filled foredeep basins generated in the front of the
31 main thrust units of the CZ. In this zone, the Variscan deformation occurred during the upper Carboniferous and
32 gave rise to thin-skinned tectonics, with several large thrust units and associated folds (Fig. 1); the units were
33 emplaced in a sequence towards the foreland. The deformation occurred under shallow crustal conditions, so that
34 diagenetic conditions are dominant in the zone and absence of cleavage in the rocks is also dominant.
35 Nevertheless, there are several areas of the CZ where cleavage and very low- or low-grade metamorphism are

36 present. One of these areas is the southeastern sector of the Cantabrian Zone. It is a foreland basin that occupies
37 the core of the Ibero-Armorican Arc and has undergone a complex history of sedimentation, deformation,
38 metamorphism and, to a lesser extent, magmatism.

39 The present study aims to present a model of tectonothermal evolution for the core of the Ibero-Armorican
40 arc based on conodont colour alteration index (CAI), the Kübler index (KI) of illite, the Árkai index (AI) of
41 chlorite, the analysis of clay minerals and the rock cleavage development.

42 **2 Geological setting**

43 The southeastern sector of the Cantabrian Zone is made up of two units: the Pisuerga-Carrión unit (PCU) and the
44 Valsurbio unit (VU) (Fig. 1). As a consequence of its location in the core of the Ibero-Armorican arc, the PCU
45 has been thrust over successively by the VU, the Central Coal Basin, the Ponga unit and the Picos de Europa unit
46 (Fig. 1). Thus, the PCU operated as a foreland basin during a great part of the history of the Variscan
47 deformation. This history involved the accumulation of a great thickness of synorogenic Carboniferous
48 sediments, corresponding to clastic wedges associated with the exhumation of the thrust units.

49 The VU is located to the south of the PCU. Marine facies occur in both units, but from the Emsian, the
50 sediments in the latter unit were deposited in deeper waters than those in the former unit. The VU represents an
51 extension of the southern part of the CZ, and **the Devonian succession of both is comparable** (Koopmans, 1962).
52 The units **within the PCU** containing Silurian-Devonian rocks have been interpreted as transported from internal
53 areas of the orogenic belt, specifically from the southeastern extension of the Westasturian-Leonese Zone,
54 currently hidden under the Mesozoic-Cenozoic cover of the Duero basin, and located to the south of the VU
55 (Frankenfeld, 1983; Marquínez and Marcos, 1984; Rodríguez Fernández and Heredia, 1987; Rodríguez
56 Fernández, 1994). These units were named ‘Palentine nappes’ by Rodríguez Fernández and Heredia (1987). The
57 PCU and the VU are separated by the León fault (also called ‘Ruesga fault’ in the study area) (Fig. 2), that
58 **crosses** most of the Cantabrian Zone and whose meaning is controversial (Alonso et al., 2009 **and references**
59 **therein**).

60 The oldest sediments of the study area are Silurian (Wenlock-Pridoli) sandstones and lutites. The Devonian
61 rocks consist of an alternation of carbonate and siliciclastic formations with the facies differences cited above.
62 Mississippian rocks are mainly limestones in the lower part, especially in the VU; upwards a mostly turbiditic
63 sequences appears with common olistoliths in the northern sector and some carbonate levels. The Pennsylvanian
64 succession is dominantly siliciclastic, with a thickness of several thousand meters and synorogenic character. In
65 relation to this synorogenic sedimentation, several syntectonic unconformities have been described, among
66 which the Curavacas unconformity (early Moscovian) can be highlighted by its structural significance (Van
67 Veen, 1965; Lobato, 1977; Alonso and Rodríguez Fernández, 1983; Martín-Merino et al., 2014).

68 The first deformation events were pre-Curavacas (prior to or earliest Moscovian) and involved the
69 emplacement of the Palentine nappes and the VU. Two generations of thrusts **and associated folds** occurred
70 during this episode (Rodríguez Fernández, 1994), which translated sequences northwards. Further, some back
71 thrusts and normal faults occurred.

72 The post-Curavacas deformation events involved the development of several generations of thrusts and
73 high-angle reverse faults, folds, cleavages and normal faults. Some thrusts have a trend approximately parallel to
74 the basal thrust of the Ponga unit and are probably related to the emplacement of this thrust unit (Rodríguez

75 Fernández and Heredia, 1987), which occurred during the late Moscovian. In the same episode that involved the
76 emplacement of the Picos de Europa thrust unit during the Kasimovian-Gzhelian (Merino-Tomé et al. 2009), N –
77 S shortening occurred in the study area, involving the development of thrusts, high angle reverse faults and the
78 reactivation of older faults with a movement dominantly southward (Maas, 1974). In addition, upright folds with
79 E – W axial trace developed; among them, the Curavacas-Lechada syncline is remarkable for its notable
80 dimensions (Savage, 1967; Lobato, 1977; Rodríguez Fernández, 1994).

81 Several cleavages have been recognised in the study area. Among them, a gently dipping cleavage
82 crosscutting folds is the most relevant and has been described by various authors (Van Veen, 1965; Savage,
83 1967; Lobato, 1977; Van der Pluijm et al., 1986; Rodríguez Fernández, 1994; Marín, 1997; García-López et al.,
84 2007; among others).

85 A subsequent N-S shortening episode occurred during the Alpine deformation. It involved tightening of
86 folds, local development of crenulation cleavage and reactivation of some faults. It is responsible for the dome
87 geometry of the VU (Marín et al., 1995; Marín, 1997). Another post-Variscan structure of the study area is the
88 Ventaniella fault, which traverses the whole Cantabrian Zone in a NW – SE direction. It is essentially a dextral,
89 strike-slip fault with a net-slip of 4-5 km (Julivert et al., 1971) whose activity began in the Permian and
90 continues to the present (López-Fernández et al., 2002, 2004).

91 Outcrops of intrusive igneous rocks are common in the PCU, and their knowledge is important to
92 understand the tectonothermal evolution of this unit. Among these rocks, three granodioritic stocks (Pico Iján,
93 Peña Prieta and Pico Jano; Fig. 2) and many small outcrops can be distinguished. The latter are mainly
94 concentrated in the southern half of the unit.

95 The stocks of Pico Iján, Peña Prieta and Pico Jano dominantly have granodioritic composition and their
96 intrusion was favoured by the existence of faults (Suárez and García, 1974; Corretgé and Suárez, 1990), having
97 developed a notable aureole of contact metamorphism in the case of the Peña Prieta stock. The porphyroblasts in
98 this aureole are post-tectonic relative to the gently dipping cleavage (Gallastegui et al., 1990; Rodríguez
99 Fernández, 1994). The U/Pb age of the Peña Prieta granitoid is Cisuralian (292±2/-3 Ma after Valverde-Vaquero
100 et al., 1999), and the Pico Iján granitoid is nonconformably covered by Lower Triassic rocks. The large number
101 of small outcrops of igneous rocks that exist in the southern half of the unit are concentrated in two areas (one in
102 the eastern part and another in the western part) joined by a band whose outcrops of igneous rocks have been
103 related to the León fault (Corretgé et al., 1987; Suárez and Corretgé, 1987; Corretgé and Suárez, 1990). All these
104 southern outcrops have been in general related to fractures and appear as small stocks, probably apophyses of
105 bigger bodies in depth, and as sills or dikes. Their composition is varied and ranges from granodioritic to
106 gabbroic. In some cases, they developed ore bodies close to their contacts (Martín-Izard et al., 1986).

107 Earlier metamorphic studies in the Cantabrian zone using CAI and/or KI methods have shown the existence
108 of areas with very low- or low-grade metamorphism in the PCU and the VU (Raven and van der Pluijm, 1986;
109 Keller and Krumm, 1993; Marín et al., 1996; Marín, 1997; Köberle et al., 1998; García-López et al., 1999, 2007,
110 2013; Bastida et al., 2002; Clauer and Weh, 2014; among others). Similar results have been obtained for the
111 southern part of the study area using coal rank and vitrinite reflectance (Colmenero and Prado, 1993; Llorens et
112 al., 2006; Colmenero et al., 2008; Clauer and Weh, 2014). This metamorphism has been described as associated
113 with a late-orogenic extensional event and with the corresponding cleavage (García-López et al., 1999, 2007,
114 2013; Bastida et al., 2002). Analysis of ore deposits and of the tectonothermal evolution in the neighbouring unit

115 of the Picos de Europa has defined a subsequent hydrothermal episode during the Permian (Gómez-Fernández et
 116 al., 1993, 2000; Bastida et al., 2004). Brime and Valín (2006) have suggested a hydrothermal origin for mineral
 117 associations with chloritoid and pyrophyllite found in samples of pelitic rocks collected in the study area. K-Ar
 118 dating of illite in samples collected in the southern part of the study area, identified four thermal episodes
 119 (Clauer and Weh 2014), namely at: (1) 293 ± 3 Ma (Cisuralian), (2) 268 ± 6 Ma (Guadalupian), (3) 243 ± 5 Ma
 120 (middle Triassic), and (4) 175 ± 6 Ma (early-middle Jurassic). From apatite fission tracks and zircon (U-Th)/He
 121 ages in samples of Westphalian (Bashkirian-Moscovian) sandstones collected in the eastern part of the PCU,
 122 Fillon et al. (2016) obtained ages of cooling below $\approx 180^\circ\text{C}$ of 37-39 Ma and below $\approx 110^\circ\text{C}$ of 28-29 Ma. They
 123 inferred Cenozoic erosion of a rock thickness between 6.4 and 8 km (assuming a steady-state geothermal
 124 gradient of 25°C km^{-1}).

125 3 Methods

126 3.1 X-ray diffraction

127 A total of 297 mudrocks from various localities (Fig. 2) were studied by X-ray diffraction (XRD) analysis in
 128 order to determine their phyllosilicate mineralogy, Kübler Index (KI) of illites, and Árkai Index of chlorites (AI).
 129 Preparation of samples and methods for XRD analysis follow the methods described in Brime et al. (2003)

130 Reaction progress in illitic minerals (*sensu* Środoń 1984) has been widely used to assess the evolution of
 131 pelitic lithologies during diagenesis and low-grade metamorphism. Prograde changes can be identified by use of
 132 the Kübler Index technique (illite “crystallinity”, see Guggenheim et al. 2002) involving quantification of the
 133 width of the 10\AA peak of illite. This is an indirect measure of lattice reorganization and thickening of illite
 134 crystals (Kisch 1983; Merriman and Peacor 1999) with increasing grade. The Kübler Index (KI) is expressed in
 135 $\Delta^\circ 2\theta$ to minimize variations caused by differences in recording conditions. For this study the KI was measured
 136 using a laboratory procedure similar to that outlined by the IGCP 294 working group (Kisch, 1991). The
 137 numerical KI value decreases with improving “crystallinity” and is expressed as small changes in the Bragg
 138 angle $\Delta^\circ 2\theta$, using Cu $K\alpha$ radiation.

139 The transient zone between diagenesis and metamorphism (the anchizone of Kübler, 1967) is defined by KI
 140 values between 0.42° and $0.25^\circ \Delta^\circ 2\theta$ respectively (Kisch, 1991). The values obtained in our laboratory were
 141 correlated with the Kübler scale using a calibration curve based on data obtained from polished slate standards
 142 kindly provided by H. Kisch. The diagenetic zone has been subdivided in shallow ($\text{KI} > 1^\circ \Delta^\circ 2\theta$) and deep (1.0°
 143 $> \text{KI} > 0.42^\circ \Delta^\circ 2\theta$), using the terms proposed by the IUGS Subcommittee on the Systematics of Metamorphic
 144 rocks (Árkai et al., 2007). Following Merriman and Peacor (1999) we have divided the anchizone into low (0.42
 145 $< \text{KI} < 0.30^\circ \Delta^\circ 2\theta$) and high ($0.30 < \text{KI} < 0.25^\circ \Delta^\circ 2\theta$).

146 Crystallinity index standards (CIS, Warr and Rice 1994) have also been used to compare the results thus
 147 obtained with other published results using that scale. KI values obtained in this work could be converted to the
 148 CIS scale by using the calibration equation:

$$149 \text{KI}_{\text{CIS}} = 1.505\text{KI}_{\text{this work}} - 0.046 \quad (R^2 = 0.996). \quad (1)$$

150 For the problems involved in the use of the CIS scale to assess metamorphic grade see Brime (1999) and
 151 Kisch et al. (2005).

152 The KI method does not allow temperature constraints to be placed on the upper and lower boundaries of
153 the anchizone and it is more likely to be a measure of reaction progress than of the thermodynamic equilibrium
154 achieved (Essene and Peacor, 1995). However, this method, in combination with others such as fluid inclusions
155 or reflectance of carbonaceous material, indicates that the transition diagenesis–anchizone could be correlated
156 with a temperature of 230 ± 10 °C, whereas the limit anchizone–epizone would be at 300 ± 10 °C (Müllis, 1979;
157 Frey et al., 1980; Frey, 1987; Von Gosen et al., 1991; Müllis et al., 1995; Merriman and Frey, 1999; Ferreiro
158 Mählmann et al., 2002; Müllis et al., 2002).

159 The presence of illite/smectite (I/S) and paragonite (Pg) and paragonite/muscovite (Pg/Ms) hampers
160 determination of KI of many samples. However, pro-grade changes can also be identified by use of the Árkai
161 Index technique (of chlorite “crystallinity”, see Guggenheim et al., 2002) involving quantification of the width of
162 the 14Å or 7Å peaks of chlorite (Árkai, 1991, Meunier, 2005). The Árkai Index (AI) was determined in the (002)
163 peak using the same instrumental conditions as those for KI measurements. The anchizone limits have been
164 established using samples free of I/S, Pg-Pg/Ms in which the KI measured in the air dried samples has been
165 calibrated with Kisch standards. The AI was measured in the same samples and the regression line obtained
166 allowed the delimitation of the upper and lower anchizone limits using chlorite for AI values of 0.234 and 0.135
167 $\Delta^{\circ}2\theta$ respectively. It should be noted that AI values are smaller than the corresponding KI and the method is
168 therefore slightly less sensitive than KI method.

169 **3.2 Conodont colour alteration index (CAI)**

170 Colour changes in conodont elements are related to the progressive and irreversible alteration of the amounts of
171 organic matter within their apatite composition. The CAI method is based on analysis of the colour changes that
172 the conodonts undergo in response of the organic matter to a temperature increase with time. These changes
173 permit construction of a scale of CAI values with eight units that allows the use of the conodonts as maximum
174 paleothermometers for a temperature interval of between 50 and 600°C (Epstein et al., 1977; Rejebian et al.,
175 1987). It is used mainly in carbonate rocks. Besides colour changes, apatite textural alteration also takes place
176 and can provide complementary information about the thermal conditions. In the present paper the terminology
177 of Rejebian et al. (1987) and García-López et al. (1997, 2006) is used for the textural description of conodonts.
178 In agreement with Rejebian et al. (1987), well preserved conodonts and high CAI values with a wide dispersion
179 are indicative of contact metamorphism. Furthermore, coarse recrystallization and corrosion are related to
180 hydrothermal processes.

181 Samples were collected from the Pisuerga-Carrión and Valsurbio units. CAI values are based on 5 kg
182 samples of limestone that were treated with 6% acetic acid solution. Unfortunately, recovery of conodonts from
183 Carboniferous rocks was hindered in some areas by their dominantly siliciclastic character. Sampling was
184 complemented with specimens from collections housed at the University of Oviedo (Spain) and those of the
185 National Museum of Natural History at Leiden (Netherlands) and Institut und Museum für Geologie und
186 Paläontologie in Göttingen (Germany) (Fig. 2). 213 positive samples, corresponding to an age interval from the
187 Pridoli to Ghzelian, were analyzed for CAI determination (Appendix 1 in the supplementary material).

188 The methodology involved in CAI determination can be found in García-López et al. (1997) and Bastida et
189 al. (1999). Several CAI values were obtained from most samples and the mean of CAI values have been
190 determined for each of them in order to tentatively contour CAI values. Samples with a range higher than 1.5

191 have not been used to obtain mean CAI values and temperatures. The interpretation of the results is mainly based
192 on the analysis of the CAI isograds and their relationship to the stratigraphic contacts and the main structures of
193 the study area.

194 For the metamorphic zonation from CAI data, we use the terminology described by García-López et al.
195 (2001), that involves a division in diacaizone ($CAI < 4$), ancaizone ($4 \leq CAI \leq 5.5$) and epicaizone ($CAI > 5.5$).

196 Temperature ranges of the CAI values were obtained from the Arrhenius plot presented by Epstein et al.
197 (1977) and Rejebian et al. (1987). The maximum possible heating time is the age of the rock. Nevertheless, it is
198 possible to place greater limits on this maximum time (García-López et al., 2013). According to the Arrhenius
199 plot a minimum temperature is required to obtain a specific CAI value. For example, in a rock with an age of 400
200 Ma (Devonian), development of $CAI = 5$ requires at least 290°C (point A in Fig. 3). Then, it can be assumed that
201 a temperature $< 290^{\circ}\text{C}$ does not contribute to generate a $CAI = 5$. Hence, to produce a given CAI, the maximum
202 time of heating begins when the rock reaches the minimum temperature necessary to produce that CAI, and it
203 ends when the rock cools down and the temperature becomes lower than this minimum value. **Although the**
204 **heating time can be slightly different depending on the geological location of the samples,** we consider that the
205 main heating time corresponds to a late-Variscan period that began at the boundary Kasimovian-Gzhelian and
206 ended at the beginning of the Triassic (heating time of about 50 Ma); **this agrees with the age of the**
207 **metamorphism analyzed below and the igneous rocks.** The hydrothermal post-Variscan episodes described by
208 Clauer and Weh (2014) and the Alpine **exhumation temperatures** (mainly Cenozoic) analyzed by Fillon et al.
209 (2016) **probably involved lower temperatures than those reached in the late-Variscan event, in which magmatism**
210 **and cleavage development are more intense. It must be taken into account that in** rocks undergoing more than
211 one heating period, the period to be considered for the development of the CAI is the one which generated higher
212 temperatures. Anyway, due to the geometry of the CAI curves in the Arrhenius plot, for heating intervals such as
213 those involved in the present case, an error of a few Ma in the maximum time of heating has little influence on
214 the results. According to Patrick et al. (1985) and Rejebian et al. (1987) the minimum time of heating assumed
215 here is of 1 Ma.

216 3.3 Cleavage

217 Development of cleavage requires mineralogical and **microstructural changes due to ductile deformation,**
218 involving mechanisms, such as pressure solution, which require a minimum temperature of about 200°C for
219 cleavage development in pelitic rocks and 175°C in limestones (Groshong et al. 1984). Thus widespread
220 presence of cleavage occurs below a certain crustal level (minimum overburden of 5-7 km; Engelder and
221 Marshak, 1985). Furthermore, the relations between folds and cleavages and the overprinting relations between
222 cleavages, play an important role in defining deformation events (Passchier and Trouw, 2005). In addition,
223 cleavage is also a key structure to establish chronological relations between metamorphic crystallization and
224 deformation.

225 In the context of the study area, we call tectonothermal event to a deformational event with cleavage
226 development and associated metamorphic conditions, and use the term thermal event for metamorphic conditions
227 without cleavage development.

228 4 Results and interpretation

229 In order to facilitate description, the samples have been **mainly** grouped in the following areas, namely Liébana,
230 Valdeón, Yuso-Carrión, Pisuerga, Riaño-Cervera and Valsurbio (Fig. 4) (cf. Martín-Merino et al., 2014).

231 4.1 Clay minerals

232 4.1.1 Clay mineral assemblages

233 Mineralogical analysis of the <2 µm fractions shows that dioctahedral K- rich mica-like structures (referred to as
234 illite or muscovite, I-Ms) is present in all the samples with the majority containing also chlorite (Chl) (Fig. 5).
235 Chlorites have poorly developed 14 Å peaks, indicating high iron content suggestive of chamositic compositions
236 (Moore and Reynolds, 1997). Other phases such as ordered illite/smectite (I/S) or paragonite (Pg) and mixed
237 layers paragonite/muscovite (Pg/Ms) are also common. Asymmetry of peaks and sample behaviour after
238 glycolation indicate the presence of ordered illite/smectite (I/S). Absence of random I/S indicate that zone 3 of
239 Eberl (1993) has been reached, suggesting that temperatures exceeded 100°C. Kaolinite (Kln) and pyrophyllite
240 (Prl) may also be present in some samples and are abundant in a few samples. In addition, chloritoid (Cld) is also
241 present and widespread in the study area. However it is more abundant in samples close to the intrusions and/or
242 faults in which case is found together with chlorite and Pg + Pg/Ms. Only in samples to the E (Pisuerga Area),
243 where it is not as abundant, it may be associated with Prl, Kln or I/S. Finally chlorite/vermiculite mixed
244 layer(C/V) and stilpnomelane (Stp) have been found, in small amounts, in a few samples, and are restricted to
245 samples to the E Pisuerga and E Yuso-Carrión areas.

246 The I/S is more abundant to the N and E (Valdeón, Liébana, and eastern part of the Pisuerga and Yuso-
247 Carrión areas) and Kln presence is almost restricted to samples to the E (Pisuerga and eastern part of the Yuso-
248 Carrión areas). Prl is common in samples from the central and northeastern parts (Liébana and Pisuerga areas,
249 and eastern part of the Yuso Carrión area) (Fig. 5). Quartz, calcite, feldspars and goethite were accessory phases
250 recognized in some samples.

251 In general the assemblages found are, in order of abundance of the most frequent phase besides illite ($n =$
252 291):

253 I + **Chl** ($n = 215$) ± Pg ± Pg/Ms ± Cld ± I/S ± [C/V] ± [Prl] ± [Kln] ± [Stp]

254 I + **Pg** + **Pg/Ms** ($n = 162$) ± Chl ± Cld ± [I/S] ± [Prl] ± [C/V] ± [Kln] ± [Stp]

255 I + **I/S** ($n = 112$) ± Chl ± Kln ± Prl ± C/V ± Pg ± Pg/Ms ± C/V ± [Cld] ± [Stp]

256 I + **Cld** ($n = 93$) ± Chl ± Pg ± Pg/Ms ± I/S ± [C/V] ± [Prl] ± [Kln] ± [Stp]

257 I + **Prl** ($n = 56$) ± I/S ± Chl ± Pg ± Pg/Ms ± C/V ± [Cld] ± [Kln] ± [Stp]

258 I + **C/V** ($n = 48$) ± I/S ± Chl ± Pg ± Pg/Ms ± Kln ± Prl ± Cld ± [Stp]

259 I + **Kln** ($n = 39$) ± I/S ± Chl ± C/V ± [Prl] ± [Cld] ± [Pg] ± [Pg/Ms] ± [Stp]

260 4.1.2 Kübler Index

261 As mentioned above, determination of KI has been hampered by the presence in some samples of certain types
262 of I/S and big amounts of Pg or Prl, in relation to the amount of illite, that interfere with the 001 peak of illite,
263 therefore rendering their KI values useless for grade determination using KI, even in the glycolated state. As a

264 result, 23 (indicated in *italics* in Appendix 2 in the supplementary material) of the 291 samples studied yielded
 265 doubtful KI values (Figs. 6, 7; Appendix 2 in the supplementary material). They are **included**, nevertheless, as
 266 they indicate maximum value of the KI.

267 Grade ranges from deep diagenetic to epizonal, but deep diagenetic and mainly low anchizonal metapelites
 268 are predominant in most of the areas (Figs. 6 and 7). Expandability of the 10 Å peak is only lost at the high
 269 anchizone to epizone boundary. Deep diagenetic areas can be found to the north (Liébana and Valdeón areas).
 270 The Riaño-Cervera area is mainly low anchizonal with a few samples being diagenetic or deep anchizonal. In the
 271 Pisuerga area, the grade ranges from deep diagenetic to low anchizonal (Figs. 6, 7). Higher grade (epizonal)
 272 samples may appear in any formation and they are more abundant in the western part of the Yuso-Carrión area,
 273 where **the Peña Prieta granodiorite** is located, and in the Devonian of the Valsurbio area (Fig.7). In both cases, it
 274 is in those high grade samples where chloritoid is more abundant (Fig.6).

275 Work in progress on the variation of the chemical composition of the phyllosilicates of the study area
 276 allowed estimation of temperatures using Battaglia's (2004) approach based in the variation in the chemical
 277 composition of illites. Temperatures obtained are in the range 230-280°C, consistent with the anchizonal KI
 278 values of the analyzed samples. The observed deficit in layer charge (Brime and Valín, 2006) is characteristic of
 279 anchizonal K white micas (Hunziker et al., 1986; Livi et al., 1997; Merriman and Peacor, 1999; Árkai, 2002;
 280 Árkai et al., 2003).

281 4.1.3 Árkai Index

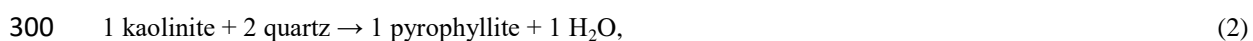
282 **The Árkai Index** has been measured in 118 samples, most if not all of them, containing various amounts of I/S
 283 and/or Pg, Pg/Ms. Of them, 40 yielded diagenetic values, 63 low anchizonal values, 14 high anchizonal values
 284 and just one epizonal value. Distribution of these values can be seen in Fig. 6. In those cases in which KI and AI
 285 have been determined, the correlation of the grade indicated by both **indices** is good ($r = 0.65$; significance level
 286 0.1% $r_{60} = 0.41$) suggesting that both phases were formed under the same conditions, and supporting the
 287 reliability of the AI as indicator of grade in those cases in which it is the only index available (Árkai et al., 1995).

288 The existence of some discrepancies between KI and AI may be caused by the presence of small amounts
 289 of I/S or Pg that alters the width of the illite peaks. However, those discrepancies are always small and are
 290 usually in samples at the boundary between metamorphic grade zones (Appendix 2 in the supplementary
 291 material).

292 4.1.4 Mineral distribution in relation with grade

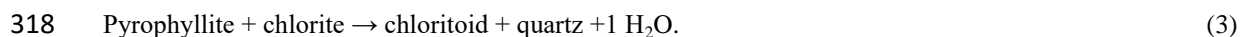
293 Kaolinite is present in deep diagenetic samples and also in some low anchizonal ones. Maximum **stability**
 294 **temperature** of Kln is 270°C, according to laboratory experiments (Velde, 1992) and therefore in agreement with
 295 its presence in the anchizonal samples. Paragonite, apart from its presence in deep diagenetic samples, is more
 296 frequently present in the anchizone and some epizonal samples (Figs. 5 and 6). Pyrophyllite is more abundant in
 297 samples from the anchizone but it can also be present in diagenetic samples.

298 The widespread occurrence of Kln and quartz in the diagenetic rock samples may provide the starting
 299 material for the formation of Prl by the reaction



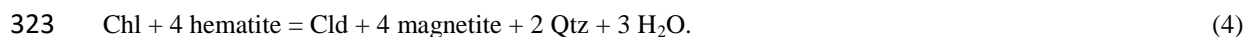
301 as suggested in the Glarus Alps by Frey (1978), who considered Prl an indicator of anchizone regional
 302 conditions. In fact of the 53 samples in which Prl is present, Kln is found, and in very small amounts, in only 8
 303 of them. However, the stability field of Prl is strongly influenced by water activity, and thus the formation
 304 temperature could be notably lower (Thompson, 1970; Winkler, 1979; Hemley et al., 1980). Its presence in
 305 diagenetic samples is not uncommon and could be due to the influence of magmatic fluids (Hosterman et al.,
 306 1970; Kisch, 1987). According to Kisch (1987), Prl appears in regional terrains only in the anchizone but in
 307 areas of intrusive activity it may appear in lower grade zones. Therefore presence of Prl in samples with
 308 diagenetic KI/AI values, as in the eastern part of the Liébana and Yuso Carrión areas, could be regarded as
 309 evidence for high geothermal gradients or magmatic heating.

310 Chloritoid is abundant in samples from the high anchizone to epizone (southeastern Valsurbio area and
 311 western Yuso Carrión area), but it can also be present, in smaller amounts, in low anchizone (1, 3W, 4E, 4W,
 312 5E, 5W) and even diagenetic samples (eastern Liébana, Pisuerga and Riaño-Cervera areas). Cld is Fe rich. The
 313 average Mg/(Fe+Mg) found is < 0.12 (Brime and Valín, 2006) similar to that of pelites subjected to intermediate
 314 *P/T* conditions. It is noteworthy that when this phase is present in the samples (a total of 93 samples have Cld),
 315 Prl is absent, or in very minor amounts in a few samples (10 in total), indicating that it could have been formed
 316 according to the reaction originally proposed by Zen (1960), which is generally accepted for the formation of
 317 Cld during metamorphism of aluminous pelites (Theye et al. 1992):

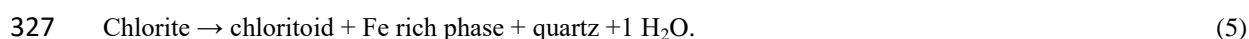


319 The absence of Cld in the eastern part of the Yuso Carrión area where Prl is abundant, together with Chl,
 320 could indicate that the temperature required for its formation by reaction (3) has not been reached.

321 Presence of some Fe oxides has been detected in samples from the study area. Therefore more Cld could be
 322 produced by the reaction suggested by Bucher and Frey (1994):



324 However, it has been observed in thin sections that occurrence of Prl is almost restricted to veins and
 325 fracture zones, suggesting that Cld could have been formed during the hydrothermal alteration of the pelites
 326 following the reaction proposed by Phillips (1988):



328 Presence of Cld in the anchizone has been discussed by Kisch (1983), who concluded that Cld cannot
 329 unequivocally be regarded as an indicator of the beginning of the epizone, as previously suggested, because there
 330 are occurrences in the anchizone (Árkai et al., 1981). In the study area, Cld is more abundant in the epizonal
 331 samples of the Valsurbio (6) and W Yuso-Carrion (3W) areas, but it is also present in low anchizone and a few
 332 deep diagenetic samples from the Riaño Cervera (5E), Pisuerga (4E) or Valdeón (2) areas, thus corroborating the
 333 conclusion of Kisch (1983).

334 Chloritoid and Prl are widespread in virtually all rock types and grade conditions (Appendix 2 in the
 335 supplementary material). This occurrence could be related to basin wide alteration by infiltrating hydrothermal
 336 fluids (Phillips, 1988; Brime and Valín, 2006). Late to post Variscan fluid flow events have been described in the
 337 other areas of the Cantabrian Zone (Ayllón et al., 2003; Gasparrini et al., 2003) and related to a more general
 338 Variscan event (Boni et al., 2000).

339 4.2 Conodont colour alteration index (CAI).

340 The CAI values are **in general** independent of the stratigraphic position of the samples (Figs. 8 and 9). **The**
 341 **Kasimovian-Gzhelian rocks show lower values, but the small number of samples makes this result not**
 342 **significant.** CAI values vary widely, ranging from 1.5 to 7.5, corresponding respectively to intervals of
 343 temperatures of < 40-60°C and 550-590°C (see Appendix 1 in the supplementary material). However, values
 344 equal to or lower than 2 are unusual, being limited to the southeastern sector of the Pisuerga-Carrión unit. Some
 345 samples with conodonts having high CAI values and a range of one and a half units, or more, are indicative of
 346 contact metamorphism and/or hydrothermal processes. Values ≥ 6 are usually found close to outcrops of igneous
 347 rocks. The upper boundary of the ancaizone (CAI = 4) corresponds to a temperature range of 190 - 225°C, while
 348 the lower limit (CAI = 5.5) corresponds to the range of 340-375°C.

349 The lack of carbonate rocks prevents in some areas the construction of a complete map of CAI isograds;
 350 however, it is possible to observe that they crosscut the trend of the Variscan structures. CAI data allow the
 351 distinguishing of the following sectors in the study area (Fig. 8):

- 352 (a) Northern sector (Liébana and Valdeón areas). This is an ancaizonal area that passes without thermal
 353 discontinuity through the basal thrust of the Picos de Europa unit. Inside this unit, the boundary
 354 ancaizone/diacaizone appears and the CAI decreases northwards (Bastida et al., 2004; Blanco-Ferrera et al.,
 355 2011).
- 356 (b) Central-eastern sector (eastern part of the Yuso-Carrión area) with dominance of ancaizonal conditions. Here,
 357 in the areas where CAI data exist, a remarkable homogeneity of CAI values appears, mainly in the Devonian
 358 rocks of the area located to the east of the Curavacas-Lechada syncline.
- 359 (c) Central and western sectors, (western part of the Yuso-Carrión and Riaño-Cervera areas) where the limited
 360 CAI data available indicate that epicaizonal areas coexist with ancaizonal areas.
- 361 (d) Southern sector. It corresponds to the VU and presents a wide area with epicaizonal conditions (García-
 362 López et al., 2013).
- 363 (e) Southeastern sector (eastern part of the Yuso-Carrión and Pisuerga areas). In this area, diacaizonal
 364 conditions are dominant, but ancaizonal and epicaizonal areas also appear. The latter areas appear adjacent
 365 to outcrops of igneous rocks. The greater variation of CAI values is found in this area, with a range from 1.5
 366 to 7.

367 The apparently chaotic distribution of CAI isograds **could be** due to a heat from subsurface intrusions at
 368 depth resulting in isotherms having complex geometry. This pattern may be related to a crustal thinning during
 369 an extensional episode and to the subsequent intrusion of igneous bodies that emplaced at different levels,
 370 generating contact metamorphism and hydrothermal fluids.

371 In general, conodonts of the study area are undeformed and well preserved. Most of them have granular
 372 texture due to apatite recrystallization under high temperature. The apatite crystals do not show preferential
 373 orientation and their size increases with temperature. The granular texture is commonly incipient for CAI values
 374 between 4 and 4.5 and is widespread for CAI values ≥ 5 . Furthermore some conodonts with CAI values between
 375 6 and 7 have coarse recrystallization, corrosion and loss of ornamentation, so that in a few cases they have lost
 376 their original morphology (“ghost conodonts”). These alterations of conodonts with CAI values ≥ 5 are
 377 indicative of contact metamorphism and hydrothermal processes. Some conodonts with CAI ≥ 4.5 present sets of
 378 parallel microfissures, probably related to the rock cleavage. Conodonts with CAI ≤ 4 have occasionally

379 unaltered surfaces, but most of them present a sugary texture (dull, frosted or pitted surfaces). The surfaces of
380 these conodonts show several types of overgrowth of apatite crystals, mainly developed in the diacaizone,
381 irrespective of the thermal conditions inside this zone; they were usually a result of apatite solution and
382 crystallization processes (Blanco-Ferrera et al., 2011).

383 4.3 Cleavage development and tectonothermal evolution

384 Two main cleavages have been found in the study area (Fig. 10). Cleavage S₁ is a rough foliation associated with
385 upright folds and trends approximately E-W; it appears mainly in the northern half of the study area. This
386 cleavage affects latest Carboniferous rocks (Kasimovian-Gzhelian age). Cleavage S₂ dips gently, crosscuts
387 earlier upright folds and is associated with the development of meter-scale open cascade folds. It is especially
388 well developed in the Curavacas-Lechada syncline (Fig. 11) and in the VU. Both cleavages appear in different
389 areas and have not been observed superimposed. The existence of two cleavages with different age suggests that
390 two tectonothermal events took place in the southeastern sector of the CZ.

391 The first event, associated with the S₁ cleavage (sub-vertical), is not well defined, since it developed in an
392 area where presence of I/S and Kln and KI and AI values indicate deep diagenesis or low anchizonal conditions,
393 and CAI values dominantly show ancaizonal conditions. According to the age of the latest rocks affected, this
394 event probably occurred during the late Gzhelian. It resulted in crustal thickening produced by the N - S
395 shortening that gave rise to the emplacement of the Picos de Europa unit, the last major Variscan thrust unit that
396 was generated in the foreland fold and thrust belt, and to the development of other thrusts and folds to the south
397 of this unit.

398 The second event produced cleavage S₂ that crosscuts the upright folds in the southern part of the study
399 area (Curavacas-Lechada syncline and the VU). Under the microscope, this cleavage shows evidences of
400 pressure solution and crystallization of oriented muscovite and chlorite with formation of chlorite-muscovite
401 porphyroblasts. X-ray diffraction indicates that the rocks affected by this cleavage present Chl + Pg-Pg/Ms
402 assemblages; KI and AI values indicate high anchizonal to epizonal conditions and CAI values indicate similar
403 conditions. The gently dipping attitude of S₂ suggests that this event was associated with an extensional
404 deformation. The event culminated with the intrusion of igneous rocks that pierced the rocks with cleavage and
405 generated a contact metamorphism associated with hydrothermal processes, as indicated by: (1) the widespread
406 presence of Cld and Prl (Fig 5; Brime and Valín, 2006) and low KI and AI values, (2) recrystallization in
407 conodonts (granular texture), (3) high CAI values in samples close to outcrops of intrusive rocks, (4) wide range
408 of CAI in some samples, and (5) irregular variation of the CAI through the area and strong corrosion in some
409 conodonts. The cleavage S₂ developed earlier than the porphyroblasts (biotite, andalusite and chloritoid) formed
410 during the contact metamorphism associated with the granodioritic stock of Peña Prieta (Gallastegui et al., 1990;
411 Rodríguez Fernández, 1994), whose age is Cisuralian (292±2/-3 Ma after Valverde-Vaquero et al., 1999). These
412 data suggest the development of a thermal event that took place near the boundary Carboniferous-Permian and
413 that progressed during the Cisuralian with the intrusion of many small igneous bodies that rose along faults
414 (Suárez and García, 1974; Corretgé and Suárez, 1990).

415 In some locations, S₂ is gently folded with local development of crenulation cleavage. This may be a result
416 of the Alpine deformation, which is the only post-Variscan compressional deformation described in the area

417 (Gallastegui, 2000 and references therein), and involved a ductile deformation that required a moderate
418 temperature and gave rise to a dome shape in the Valsurbio unit (Marín, 1997).

419 The features described above refer to penetrative structures or to the thermal history developed during the
420 last stages of the Variscan evolution. However, this evolution does not preclude the development of other
421 thermal episodes subsequently, such as the hydrothermal post-Variscan episodes described by Boni et al. (2000),
422 Mucchez et al. (2005), Gasparrini et al. (2006) and Clauer and Weh (2014).

423 5 Discussion

424 The distribution of the different grade indicators used in the study area shows, in general, an acceptable
425 correlation between them, although some discrepancies have been observed. All methods coincide in pointing
426 out the location of the areas with higher metamorphic grade, being the CAI and the AI the indicators that tend to
427 give the highest and the lowest grade respectively. All indices point to an irregular distribution of the areas with
428 very low-grade metamorphism. Diacaizonal areas are limited to the southeastern sector. A discrepancy is
429 observed in the eastern Yuso-Carrión area between clay mineral and CAI data; a notable number of CAI values
430 systematically indicate ancaizonal conditions, whereas clay assemblages with abundant I/S and Kln, KI and AI
431 indicate diagenetic conditions.

432 The correlation among the different indicators that can be used to establish the metamorphic grade is
433 challenging due to several factors, such as the different kinetics of the processes that modify the colour of the
434 conodonts and the transformation of the clay minerals and the different influence of fluids in limestones and
435 pelitic rocks. These processes could explain the discrepancies observed.

436 In the context of the Cantabrian Zone, the low-grade extensional metamorphism of the PCU extends
437 westwards and allows an elongated area to be defined that can be followed up to the Central Coal Basin (Fig. 1)
438 (Aller, 1981, 1986; Brime, 1985; Aller et al., 1987, 2005; García-López et al., 2007). The biggest width of this
439 zone is in the study area, coinciding with the core of the Ibero-Armorican arc, where a special evolution occurred
440 in the context of the CZ. The last stages of arc tightening gave rise to strong shortening with formation of folds
441 and cleavage (S_1) in the core of the arc, and the corresponding crustal thickening and heating (late Gzhelian).
442 Subsequently, a gravitational instability in this core produced an extensional episode during which low-grade
443 metamorphism and subhorizontal cleavage (S_2) crosscutting previous folds developed in some areas. This
444 evolution continued during the Cisuralian with the intrusion of igneous bodies and associated contact
445 metamorphism whose minerals post-date the S_2 cleavage. The existence of a crustal thickening followed by a
446 gravitational instability in the core of the Ibero-Armorican arc has also been proposed by other authors
447 (Gutiérrez-Alonso et al., 2004, 2011). In the Central Coal Basin, the metamorphism associated with
448 subhorizontal cleavage and crosscutting folds has been related to the possible existence of igneous bodies in
449 depth (Aller, 1986) or to the rise of fluids along faults, especially the León fault (Aller et al., 2005). In the
450 metamorphic southern part of the study area (VU), the metamorphism disappears westward, so that the adjacent
451 western unit of the Esla nappe region is not metamorphic (García-López et al., 2013; Valín and Brime,
452 unpublished data).

453 The existence of hydrothermal alteration has been suggested by Brime and Valín (2006) and Clauer and
454 Weh (2014). The common occurrence of Cld and Prl and the irregular distribution of CAI values, the wide range

455 in the high CAI values in some samples and textural alterations of conodonts agree with the occurrence of
456 hydrothermal fluids and possible subsurface igneous bodies. As for the thermal events dated by Clauer and Weh
457 (illite K-Ar; 2014), the first has an age (293 ± 3 Ma), comparable to that of the Peña Prieta **granitoid**, and the
458 others (Guadalupian, middle Triassic and early-middle Jurassic) are probably related to the crustal extension
459 associated with the Basque-Cantabrian basin. Specific structural evidences of these three later events have not
460 been found and their temperatures were probably lower than those of the late-Variscan extensional episode,
461 which, being related to igneous intrusions, probably gave rise to the paleothermal peak.

462 The zircon (U-Th)/He ages obtained by Fillon et al. (2016) indicate that the Westphalian (Bashkirian-
463 Moscovian) rocks involved in the dating had probably a temperature above 180°C up to 37-39 Ma ago (Eocene).
464 This is consistent with the occurrence of Alpine ductile deformation, which resulted in a local crenulation
465 cleavage.

466 **6 Conclusions**

467 Study of the low-grade metamorphic rocks and associated structures in the south-eastern sector of the CZ has
468 allowed a model for the tectonothermal evolution of the core of an arcuate orogenic belt to be developed. This
469 core, although it is a part of a foreland fold and thrust belt where diagenetic conditions are dominant, portrays a
470 complex evolution due to its special location inside the belt. It was thrust during the Carboniferous by large units
471 from south, west and north, which resulted in a great accumulation of syntectonic sediments, and development of
472 unconformities and structures. The latter arose as a result of compression in different directions that also
473 generated a crustal thickening. The emplacement of the last thrust unit (Picos de Europa unit) produced a N – S
474 shortening that generated thrusts and associated folds. Shortly afterwards, upright folds with E – W trend and
475 associated cleavage (S_1) developed, mainly in the northern part of the sector. The ductile deformation occurred
476 under thermal conditions which reached the anchizone and the ancaizone in some areas. This represents the first
477 tectonothermal event registered in the southeastern sector of the CZ.

478 At the end of the Variscan deformation, gravitational instability gave rise to an extensional episode and the
479 corresponding crustal thinning. During this event an increase in the thermal gradient enabled ductile deformation
480 and low-grade metamorphism to take place in some areas (second tectonothermal event), mainly in the central
481 part (Curavacas-Lechada syncline) and the southern part (Valsurbio unit) of the sector. The ductile deformation
482 produced gently dipping cleavage (S_2) crosscutting earlier upright F_1 folds. Some small open cascade folds were
483 also produced. The metamorphism reached epizonal and epicaizonal conditions during this event. The process
484 culminated in the Cisuralian with the intrusion of igneous rocks and the development of contact metamorphism
485 around the larger igneous bodies. In the case of Peña Prieta granodiorite, post S_1 andalusite porphyroblasts
486 developed. Hydrothermal fluids were common during this extensional episode, resulting in the development of
487 Prl and Cld , and textural alteration and high CAI dispersions in conodont samples.

488 As a whole, the metamorphic grade is independent of the stratigraphic location of the samples and the trend
489 of the main structures, indicating the late-orogenic character of the tectonothermal events. The thermal level
490 decreases progressively northwards inside the adjacent Picos de Europa unit. On the other hand, the
491 metamorphism associated with the extensional episode in the PCU is extended westwards as an elongated area
492 whose development was probably favoured by the rise of fluids along faults, especially along the León fault.

493 With the development of the adjacent Basque-Cantabrian basin, the extensional regime extended during the
494 Mesozoic, with the probable occurrence of hydrothermal processes. The temperature of the rocks was probably
495 important during Cenozoic times ($> 180^{\circ}\text{C}$ until the late-Eocene after Fillon et al., 2016, in the eastern part of the
496 study area), so that the Alpine deformation generated locally some ductile deformation with crenulation cleavage
497 affecting the S_2 cleavage.

498 The evolution described above is summarized in Table 1.

499

500 **Acknowledgements.** This paper is dedicated to the memory of Andrés Pérez Estaún in recognition to his major
 501 contribution to the study the geology of the Variscan belt in Spain and his pioneer work on the low-grade
 502 metamorphism of the area, and in gratitude for fruitful cooperation over a period of many years. The present
 503 paper has been supported by the CGL2015-66997-R project funded by the **Ministerio de Economía y**
 504 **Competitividad of Spain.** The authors acknowledge Dr. Robin Offler who read an earlier version of this paper
 505 and suggested improvements. Susana García-López acknowledges the cooperation of C. F. Winkler Prins from
 506 the National Museum of Natural History (Leiden, Netherlands) and H. Jahnke from the Institut und Museum für
 507 Geologie und Paläontologie (Göttingen, Germany) **for providing** access to the Cantabrian conodont collections
 508 of these institutions. **We thank Tom Blenkinsop, Josep Poblet and an anonymous referee for useful suggestions**
 509 **for improving the manuscript.**

510 **References**

- 511 Aller, J.: La estructura del borde sudoeste de la Cuenca Carbonífera Central (Zona Cantábrica, NW de España),
 512 *Trabajos de Geología*, 11, 3-14, 1981.
- 513 Aller, J.: La estructura del sector meridional de las unidades del Aramo y Cuenca Carbonífera Central,
 514 *Principado de Asturias, Spain*, 180 pp, 1986.
- 515 Aller, J., Bastida, B., Brime, C., and Pérez-Estaún, A.: Cleavage and its relation with metamorphic grade in the
 516 Cantabrian Zone (Hercynian of North-West Spain), *Sci. Géol. Bull.*, 40, 255-272, 1987.
- 517 Aller, J., Valín, M. L., García-López, S., Brime, C., and Bastida, F.: Superposition of tectono-thermal episodes in
 518 the southern Cantabrian Zone (foreland thrust and fold belt of the Iberian Variscides, NW Spain), *Bull. Soc.*
 519 *Géol. France*, 176, 503-514, 2005.
- 520 Alonso, J. L. and Rodríguez Fernández, L. R.: Las discordancias carboníferas de la región del Pisuerga-Carrión
 521 (Cordillera Cantábrica, NO de España). Significado orogénico, *Comptes Rendus del X Congreso*
 522 *Internacional de Estratigrafía y Geología del Carbonífero*, Instituto Geológico y Minero de España, Madrid,
 523 Spain, 533-540, 1983.
- 524 Alonso, J. L., Marcos, A., and Suárez, A.: Paleogeographic inversion resulting from large out of sequence
 525 breaching thrusts: The León Fault (Cantabrian Zone, NW Iberia). A new picture of the external Variscan
 526 Thrust belt in the Ibero-Armorican Arc, *Geologica Acta*, 7, 451-473, doi: 10.1344/105.000001449, 2009.
- 527 Ambrose, T., Carballeira, J, López Rico, J., and Wagner, R. H.: Mapa Geológico de España E. 1:50.000, Hoja N°
 528 107, *Inst.Geol. Min. España*, 1984.
- 529 Árkai, P.: Chlorite crystallinity: an empirical approach and correlation with illite crystallinity, coal rank and
 530 mineral facies as exemplified by Palaeozoic and Mesozoic rocks of northeast Hungary, *J. Metamorph. Geol.*,
 531 9, 723-734, 1991.
- 532 Árkai, P.: Phyllosilicates in very low-grade metamorphism: transformation to micas, in: Mottana A., Sassi, F. P.,
 533 Thompson J. B., Guggenheim, S. (eds), *Micas: crystal chemistry and metamorphic petrology*, Mineralogical
 534 Society of America, Blacksburg, Virginia, *Rev. Mineral. Geochem.* 46, 463-478. 2002.
- 535 Árkai, P., Horváth, Z. A., and Tóth, M.: Transitional very low-and low-grade regional metamorphism of the
 536 Paleozoic formations, Uppony Mountains, NE-Hungary: mineral assemblages, illite-crystallinity, -b0 vitrinite
 537 reflectance data, *Acta Geol. Acad. Sci. Hung.*, 24, 265-294, 1981.

- 538 Árkai, P., Sassi, F. P., and Sassi, R.: Simultaneous measurements of chlorite and illite crystallinity: a more
539 reliable tool for monitoring low- to very low grade metamorphism in metapelites. A case study from the
540 Southern Alps (NE Italy), *Eur. J. Mineral.*, 7, 1115-1128, 1995.
- 541 Árkai, P., Faryad, S. W., Vidal, O., and Balogh, K.: Very low-grade metamorphism of sedimentary rocks of the
542 Meliata unit, Western Carpathians, Slovakia: implications of phyllosilicate characteristics, *Int. J. Earth Sci.*,
543 92, 68-85, doi:10.1007/s00531-002-0303-x, 2003.
- 544 Árkai, P., Sassi, F. P., and Desmonds, J. 2007. 5. Very low- to low-grade metamorphic rocks. Recommendations
545 by the IUGS Subcommittee on the Systematics of Metamorphic rocks, Web version of 01/02/07, 2007.
- 546 Ayllón, F., Bakker, R. J., and Warr, L. N.: Re-equilibration of fluid inclusions in diagenetic-anchizonal rocks of
547 the Ciñera-Matallana coal basin (NW Spain), *Geofluids*, 3, 49-68, doi: 10.1046/J.1468-8123.2003.00048.X,
548 2003.
- 549 Bastida, F., Brime, C., García-López, S., and Sarmiento, G. N.: Tectonothermal evolution in a region with thin
550 skinned tectonics: the western nappes in the Cantabrian Zone (Variscan belt of NW Spain), *Int. J. Earth. Sci.*
551 (*Geol. Rundsch.*), 88, 38-48, doi: 10.1007/s005310050244, 1999.
- 552 Bastida, F., Brime, C., García-López, S., Aller, J., Valín, M. L., and Sanz López, J.: Tectonothermal evolution of
553 the Cantabrian Zone (NW Spain), in: *Palaeozoic conodonts from northern Spain*, editors: García-López, S.,
554 and Bastida F., *Cuadernos del Museo Geominero 1*, Inst. Geol. y Minero, Madrid, Spain, 105-23, 2002.
- 555 Bastida, F., Blanco-Ferrera, S., García-López, S., Sanz-López, J., and Valín, M.L.: Transition from diagenesis to
556 metamorphism in a calcareous tectonic unit of the Iberian Variscan belt (Central massif of the Picos de
557 Europa, NW Spain), *Geol. Mag.*, 141, 617-628, doi: 10.1017/S0016756804009653, 2004.
- 558 Battaglia, S.: Variations in the chemical composition of illite from five geothermal fields: a possible
559 geothermometer, *Clay Miner.*, 39, 501-510, doi:10.1180/0009855043940150, 2004.
- 560 Blanco-Ferrera, S., Sanz-López, J., García-López, S., Bastida, F., and Valín, M. L.: Conodont alteration and
561 tectonothermal evolution of a diagenetic unit in the Iberian Variscan belt (Ponga-Cuera unit, NW Spain),
562 *Geol. Mag.*, 148, 35-49, doi:10.1017/S0016756810000269, 2011.
- 563 Boni, M., Iannace, A., Bechstädt, T., and Gasparri, M.: Hydrothermal dolomites in SW Sardinia (Italy) and
564 Cantabria (NW Spain): evidence for late- to post-Variscan widespread fluid-flow events, *J. Geochem.*
565 *Explor.* 69-70, 225-228, 2000.
- 566 Brime, C.: A diagenesis to metamorphism transition in the Hercynian of north-west Spain, *Mineral. Mag.*, 49,
567 481-484, 1985.
- 568 Brime, C.: Metamorfismo de bajo grado: ¿diferencias en escala o diferencias en grado metamórfico?, *Trabajos*
569 *de Geología*, 21, 61-66, 1999.
- 570 Brime, C. and Valín, M. L.: Asociaciones con cloritoide en rocas de bajo grado metamórfico de la Unidad del
571 Pisuerga-Carrión (Zona Cantábrica, NO de España), *Macla*, 6, 105-108, 2006.
- 572 Brime, C., Talent, J. A., and Mawson, R.: Low-grade metamorphism in the Palaeozoic sequence of the
573 Townsville hinterland, northeastern Australia, *Aust. J. Earth Sci.*, 50, 751-767, doi:10.1111/j.1440-
574 0952.2003.01023.x, 2003.
- 575 Brouwer, A.: Deux facies dans le Dévonien des montagnes cantabriques meridionales, *Breviora Geológica*
576 *Astúrica*, VIII, 3-10, 1964.
- 577 Bucher, K. and Frey, M.: *Petrogenesis of Metamorphic Rocks*, 6th Edn. Springer-Verlag, Berlín, 318 pp, 1994.

- 578 Clauer, N. and Weh, A.: Time constraints for the tectono-thermal evolution of the Cantabrian Zone in NW Spain
579 by illite K-Ar dating, *Tectonophysics*, 623, 39-51, <http://dx.doi.org/10.1016/j.tecto.2014.03.013>, 2014.
- 580 Colmenero, J. R. and Prado, J. G.: Coal basins in the Cantabrian Mountains, Northwestern Spain, *Int. J. Coal*
581 *Geol.*, 23, 215-229, 1993.
- 582 Colmenero, J. R., Suárez-Ruiz, I., Fernández-Suárez, J., Barba, P., and Llorens, T.: Genesis and Rank
583 distribution of Upper Carboniferous coal basins in the Cantabrian Mountains, Northern Spain, *Int. J. Coal*
584 *Geol.*, 76, 187-204, doi:10.1016/j.coal.2008.08.004, 2008.
- 585 Colmenero, J. R., Vargas, I., García-Ramos, J. C., Manjón, M., Creapo, A., and Matas, J.: Mapa Geológico de
586 España E. 1:50.000, Hoja Nº 132, Guardo, Inst.Geol. Min. España, 1982.
- 587 Corretgé, L. G. and Suárez, O.: Igneous rocks of the cantabrian/Palentine Zone, in: Dallmeyer R. D., and
588 Martínez García, E. (eds), *Pre-Mesozoic Geology of Iberia* 72-79, Springer, Berlin, 1990.
- 589 Corretgé, L. G., Cienfuegos, I., Cuesta, A., Galán, G., Montero, P., Rodríguez Pevida, L. S., Suárez, O., and
590 Villa, L.: Granitoides de la Región Palentina (Cordillera Cantábrica, España), *Actas e Comunicações*, IX
591 *Reuniao sobre a Geologia do Oeste Peninsular* (Porto, 1985), *Memorias Univ. Do Porto*, 1, 469-478, 1987.
- 592 Eberl, D. D.: Three zones for illite formation during burial diagenesis and metamorphism, *Clays Clay Miner.*, 41,
593 26-37, 1993.
- 594 Engelder, T. and Marshak, S.: Disjunctive cleavage formed at shallow depths in sedimentary rocks, *J. Struct.l*
595 *Geol.*, 7, 327-343, 1985.
- 596 Epstein, A. G., Epstein, J. B. and Harris, L. D.: Conodont color alteration-an index to organic metamorphism,
597 Washington, D.C., *Geol. Surv. Prof. Pap.*, 995, 1-27, 1977.
- 598 Essene, E. J. and Peacor, D. R.: Clay mineral thermometry - a critical perspective, *Clays Clay Miner.*, 43, 540-
599 553, 1995.
- 600 Ferreiro Mählmann, R., Petrova, T. V., Pironon, J., Stern, W. B., Ghanbaja, J., Dubessy, J., and Frey, M.:
601 Transmission electron microscopy study of carbonaceous material in a metamorphic profile from diagenesis
602 to amphibolite facies (Bündnerschiefer, eastern Switzerland), *Schweiz. Mineral. Petrogr. Mitt.*, 82, 253-272,
603 2002.
- 604 Fillon, C., Pedreira, D., van der Beek, P., Huismans, R. S., Barbero, L., and Pulgar, J. A.: Alpine exhumation of
605 the central Cantabrian Mountains, Northwest Spain, *Tectonics*, 35, 339-356, 2016, doi:
606 10.1002/2015TC004050.
- 607 Frankenfeld, H.: El manto del Montó-Arauz; interpretación estructural de la Región del Pisuerga-Carrión (Zona
608 Cantábrica España), *Trabajos de Geología*, 13, 37-47, 1983.
- 609 Frey, M.: Progressive low-grade metamorphism of a black shale formation, Central Swiss Alps, with special
610 reference to pyrophyllite and margarite bearing assemblages, *J. Petrol.*, 19, 1, 95-135, 1978.
- 611 Frey, M.: Very low-grade metamorphism of clastic sedimentary rocks, in: Frey M. (ed), *Low temperature*
612 *metamorphism*, Blackie, Glasgow, pp 9-58, 1987.
- 613 Frey, M., Teichmüller, M., Teichmüller, R., Müllis, J., Künzi, B., Breitschmid, A., Gruner, U., and Schwizer, B.:
614 Very low grade metamorphism in external parts of the Central Alps: illite crystallinity, coal rank and fluid
615 inclusion data. *Eclogae Geol. Helv.* 73:173-203, 1980
- 616 Gallastegui, J.: Estructura cortical de la cordillera y margen continental cantábricos: perfiles ESCI-N, *Trabajos*
617 *de Geología*, 22, 9-234, 2000.

- 618 Gallastegui, G., Heredia, N., Rodríguez Fernández, L. R., and Cuesta, A.: El “stock” de Peña Prieta en el
619 contexto del magmatismo de la Unidad del Pisuergra-Carrión (Zona Cantábrica, N de España), Cuadernos do
620 Laboratorio Xeolóxico de Laxe, 15, 203-215, 1990.
- 621 García-López, S., Brime, C., Bastida, F., and Sarmiento, G. N.: Simultaneous use of thermal indicators to
622 analyse the transition from diagenesis to metamorphism: an example from the Variscan Belt of northwest
623 Spain, *Geol. Mag.*, 134, 323–334, 1997.
- 624 García-López, S., Bastida, F., Brime, C., Aller, J., Valín, M. L., Sanz-López J., Méndez, C. A., and Menéndez-
625 Álvarez, J. R.: Los episodios metamórficos de la Zona Cantábrica y su contexto estructural, *Trabajos de*
626 *Geología*, 21, 177-187, 1999.
- 627 García-López, S., Bastida, F., Aller, J., and Sanz-López J.: Geothermal palaeogradients and metamorphic
628 zonation from the conodont colour alteration index (CAI), *Terra Nova*, 13, 2, 79-83, , 2001.
- 629 García-López, S., Blanco-Ferrera, S., and Sanz-López, J.: Aplicación de los conodontos al conocimiento de la
630 evolución tectonotérmica de las zonas externas de los orógenos, *Revista Española de Micropaleontología*, 38,
631 289-298, 2006.
- 632 García-López, S., Brime, C., Valín, M. L., Sanz-López J., Bastida, F., Aller, J., and Blanco Ferrera, S.:
633 Tectonothermal evolution of a foreland fold and thrust belt: the Cantabrian Zone (Iberian Variscan belt, NW
634 Spain), *Terra Nova*, 19, 469-475, doi: 10.1111/j.1365-3121.2007.00773.x, 2007.
- 635 García-López, S., Bastida, F., Aller, J., Sanz-López, J., Marín, J. A., and Blanco Ferrera, S.: Tectonothermal
636 evolution of a major thrust system: the Esla–VU (Cantabrian Zone, NW Spain), *Geol. Mag.*, 150, 1047-1061,
637 doi:10.1017/S0016756813000071, 2013.
- 638 Gasparrini, M., Bakker, R. J., Bechstädt, Th., and Boni, M.: Hot dolomites in a Variscan foreland belt:
639 hydrothermal flow in the Cantabrian Zone (NW Spain), *J. Geochem. Explor.* 78-79, 501-507, doi:
640 10.1016/S0375-6742(03)00115-8, 2003.
- 641 Gasparrini, M., Bechstädt, Th., and Boni, M.: Massive hydrothermal dolomites in the southwestern Cantabrian
642 Zone (Spain) and their relation to the Late Variscan evolution, *Mar. Pet. Geol.*, 23, 543-568,
643 doi:10.1016/j.marpetgeo.2006.05.003, 2006.
- 644 Gómez-Fernández, F., Mangas, J., Both, R. A., and Arribas, A.: Metallogenesis of the Zn-Pb deposits of the
645 southeastern region of the Picos de Europa (Cantabria, Spain), in: Fenoll Hach-Ali, P., Torres-Ruiz J., and
646 Gervilla F. (eds), *Current research in geology applied to ore deposits*, Univ. Granada, Granada, Spain, 113-
647 116, 1993.
- 648 Gómez-Fernández, F., Both, R. A., Mangas, J., and Arribas, A.: Metallogenesis of Zn-Pb carbonate-hosted
649 mineralization in the southeastern region of the Picos de Europa (Central Northern Spain) Province: geologic,
650 fluid inclusion, and stable isotopes studies. *Econ. Geol.*, doi:95, 19-40, 10.2113/gsecongeo.95.1.19, 2000.
- 651 Groshong, Jr R. H., Pfiffner, O. A., and Pringle, L. R.: Strain partitioning in the Helvetic thrust belt of eastern
652 Switzerland from the leading edge to the internal zone, *J. Struct. Geol.* 6, 5-18, 1984.
- 653 Guggenheim, S., Bain, D. C., Bergaya, F., Brigatti, M. F., Drits, V. A., Eberl, D. D., Formoso, M. L. L., Galán,
654 E., Merriman, R. J., Peacor, D.R., Stanjek, H., and Watanabe, T.: Report of the Association Internationale
655 pour l’Etude des Argiles (AIPEA) Nomenclature Committee for 2001: order, disorder, and crystallinity in
656 phyllosilicates and the use of the “Crystallinity Index”, *Clays Clay Miner.*, 50, 406-409, 2002.

- 657 Gutiérrez-Alonso, G., Fernández-Suárez, J., and Weil, A.: Orocline triggered lithospheric delamination, in:
658 Sussman, A. J., and Weil, A. B., (eds), *Orogenic Curvature: Integrating Paleomagnetic and Structural*
659 *Analyses: Geol. Soc. Am. Special Paper 383*, 121–130, 2004.
- 660 Gutiérrez-Alonso, G., Murphy, J. B., Fernández-Suárez, J., Weil, A., Piedad Franco, M., and Gonzalo, J. C.:
661 Lithospheric delamination in the core of Pangea: Sm-Nd insights from the Iberian mantle, *Geology*, 39, 155-
662 158, doi: 10.1130/G31468.1, 2011.
- 663 Hemley, J. J., Monteya, J. W., Marinenko, J. W., and Luce, R. W.: Equilibria in the system $Al_2O_3 - SiO_2 - H_2O$
664 and some general implications for alteration mineralization processes, *Econ. Geol.*, 75, 210-228, 1980.
- 665 Heredia, N., Alonso, J. L., and Rodríguez Fernández, L. R. Mapa Geológico de España E. 1:50.000, Hoja N°
666 105, Riaño, Inst. Geol. Min. España, 1997.
- 667 Heredia, N., Navarro, D., Rodríguez Fernández, L. R., Pujalte, V., and García Mondéjar, J.: Mapa Geológico de
668 España E. 1:50.000, Hoja N° 82, Tudanca, Inst. Geol. Min. España, 1986.
- 669 Heredia, N., Rodríguez Fernández, L. R., Suárez, A., and Álvarez Marrón, J.: Mapa Geológico de España E.
670 1:50.000, Hoja N° 80, Burón, Inst. Geol. Min. España, 1991.
- 671 Hosterman, J. W., Wood, G. H., and Beryin, M. J.: Mineralogy of underclays in the Pennsylvania anthracite
672 region, U.S. Geological Survey Professional Paper 700-C, C89-C97, 1970.
- 673 Hunziker, J. C., Frey, M., Clauer, N., Dallmeyer, R. D., Friedrichsen, H., Flehmig, W., Hochstrasser, K.,
674 Roggwiler, P., and Schwander, H.: The evolution of illite to muscovite: mineralogical and isotopic data from
675 Glarus Alps, Switzerland, *Contrib. Mineral. Petrol.*, 92, 157-180, 1986.
- 676 Julivert, M.: Décollement tectonics in the Hercynian Cordillera of NW Spain, *Am. J. Sci.*, 270, 1-29, 1971.
- 677 Julivert, M. : Hercynian orogeny and Carboniferous paleogeography in northwestern Spain: A model of
678 deformation-sedimentation relationships, *Z. dt. geol. Ges.*, 129, 565-592, 1978.
- 679 Julivert, M., Ramirez del Pozo, J., and Truyols, J.: Le reseau de failles et la couverture post-hercynienne dans les
680 Asturies, in: *Histoire structurale du Golfe de Gascogne*, Publications de l'Institut Français du Pétrole,
681 Editions Tech. 2, V.3.1- V.3.34, 1971.
- 682 Julivert, J. and Navarro, D.: Mapa Geológico de España E. 1:50.000, Hoja N° 55, Beleño, Inst. Geol. Min.
683 España, 1984.
- 684 Keller, M., and Krumm, S.: Variscan versus Caledonian and Precambrian metamorphic events in the Cantabrian
685 Mountains. *Z. dt. Geol. Ges.*, 144, 88-103, 1993.
- 686 Kisch, H. J.: Mineralogy and petrology of burial diagenesis (burial metamorphism) and incipient metamorphism
687 in clastic rocks, in: Larsen G, Chilingar G. V. (eds), *Diagenesis in sediments and sedimentary rocks*, 2.
688 Elsevier, Amsterdam, pp 289-493 and 513-541, 1983.
- 689 Kisch, H. J.: Correlation between indicators of very-low grade metamorphism, in: Frey, M. (ed), *Low*
690 *temperature metamorphism*, Blackwell Science, Claridge, pp. 227-300, 1987.
- 691 Kisch, H. J.: Illite crystallinity: recommendations on sample preparation, X-ray diffraction settings and
692 interlaboratory settings, *J. Metamorph. Geol.*, 9, 665-670, 1991.
- 693 Kisch, H. J., Árkai, P., and Brime, C.: On the calibration of the illite Kübler index (illite “crystallinity”),
694 *Schweiz. Mineral. Petrogr. Mitt.* 84, 232-331, 2004.
- 695 Köberle, T, Keller, M., and Krumm, S.: Metamorphism in the southeastern corner of the Cantabrian Mountains
696 as revealed by the Upper Devonian Murcia Quartzite, *Zbl. Geol. Paläont. Teil I*, 5-6, 447-460, 1998.

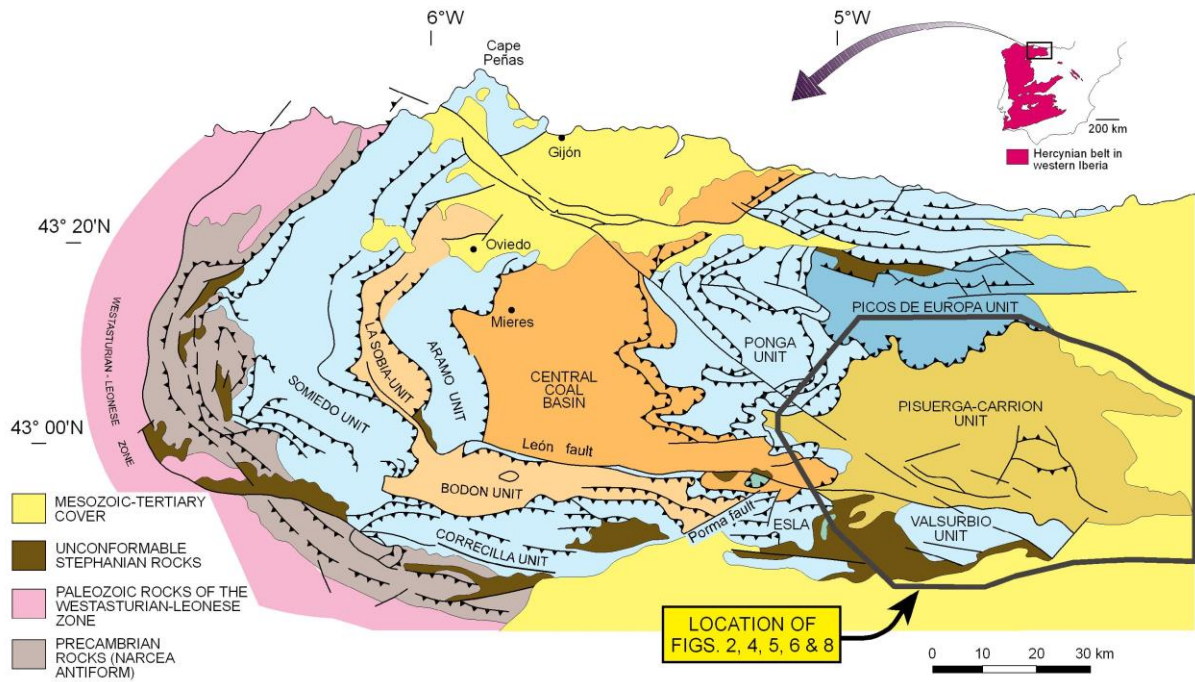
- 697 Koopmans, B. N.: The sedimentary and structural history of the Valsurvio dome, Cantabrian Mountains, Spain,
698 Leidse. Geol. Med., 26, 121-232, 1962.
- 699 Kübler, B.: La cristallinité d'illite et les zones tout à fait supérieures du metamorphism. Etages
700 tectoniques. Université Neuchâtel à la Baconnière, Neuchâtel, Switzerland, Colloques de Neuchâtel 1966,
701 105-122, 1967.
- 702 Livi, K. J. T., Veblen, D.R., Ferry, J. M., and Frey, M.: Evolution of 2:1 layered silicates in low-grade
703 metamorphosed Liassic shales of Central Switzerland, *J. Metamorph. Geol.*, 15, 323-344, 1997.
- 704 Llorens, T., Suárez-Ruiz, I., and Colmenero J. R.: Petrografía de los carbones cantabrienses (Carbonífero sup.)
705 del Grupo Cea de la Cuenca Guardo-Valderrueda (León-Palencia), *Geogaceta*, 40, 279-282, 2006.
- 706 Lobato, L.: Geología de los valles altos de los ríos Esla, Yuso, Carrión y Deva. Institución Fray Bernardino de
707 Sahagún, León (C.S.I.C.), 192 pp., 1977.
- 708 Lobato, L., Rodríguez Fernández, L. R., Heredia, N., Velando, F., and Matas, J.: Mapa Geológico de España E.
709 1:50.000, Hoja N° 106, Camporredondo de Alba, *Inst. Geol. Min. España*, 1985.
- 710 López-Fernández, C., Pulgar, J. A., Gallart, J., González-Cortina, J. M., Díaz, J., and Ruiz, M.: Actividad
711 sísmica reciente en el noroeste de la Península, 3ª Asamblea Hispano Portuguesa de Geodesia y Geofísica, 1-
712 4, Valencia, 2002.
- 713 López-Fernández, C., Pulgar, J. A., Glez.-Cortina, J. M., Gallart, J., Díaz, J., and Ruiz, M.: Actividad sísmica en
714 el noroeste de la Península Ibérica observada por la red sísmica local del Proyecto GASPI (1999-2002),
715 *Trabajos de Geología*, 24, 91-106, 2004.
- 716 Maas, K.: The geology of Liébana, Cantabrian Mountains, Spain: Deposition and Deformation in a flysch area,
717 *Leidse. Geol. Med.*, 49, 379-465, 1974.
- 718 Marcos, A. and Pulgar, J. A.: An approach to the tectonostratigraphic evolution of the Cantabrian Foreland thrust
719 and fold belt, Hercynian Cordillera of NW Spain, *Neues Jahrb. Geol. Paläontol. Abh.*, 163, 256-260, 1982.
- 720 Marín, J. A.: Estructura del domo de Valsurvio y borde suroriental de la región del Pisuerga-Carrión (Zona
721 Cantábrica, NO de España). Unpublished Ph. D. thesis, Oviedo University, 181 pp., 1997.
- 722 Marín, J. A., Pulgar, J. A., and Alonso, J. L.: La deformación alpina en el Domo de Valsurvio (Zona Cantábrica,
723 NO de España). *Revista de la Sociedad Geológica de España*, 8, 111-116, 1995.
- 724 Marín, J. A., Villa, E., García-López, S., and Menéndez, J. R.: Estratigrafía y metamorfismo del Carbonífero de
725 la zona de San Martín-Ventanilla (Norte de Palencia, Cordillera Cantábrica), *Revista de la Sociedad*
726 *Geológica de España*, 9, 241-251, 1996.
- 727 Marquínez, J. and Marcos, A.: La estructura de la unidad del Gildar-Montó (Cordillera Cantábrica), *Trabajos de*
728 *Geología*, 14, 53-64, 1984.
- 729 Martínez García, E., Marquínez, J., Heredia, N., Navarro, D., and Rodríguez Fernández, L. R.: Mapa Geológico
730 de España E. 1:50.000, Hoja N° 56, Carreña-Cabrales, *Inst. Geol. Min. España*, 1984.
- 731 Martín-Izard, A., Palero, F. J., Regillón, R., and Vindel, E.: El skarn de Carracedo (San Salvador de Cantamuda).
732 Un ejemplo de mineralización pirometasomática en el N. de la provincia de Palencia, *Studia Geologica*
733 *Salmanticensis*, XXIII, 171-192, 1986.
- 734 Martín-Merino, G., Fernández, L. P., Colmenero, J. R., and Bahamonde, J. R.: Mass-transport deposits in a
735 Variscan wedge-top foreland basin (Pisuerga area, Cantabrian Zone, NW Spain) , *Marine Geology*, 356, 71-
736 87, <http://dx.doi.org/10.1016/j.margeo.2014.01.012>, 2014.

- 737 Merino-Tomé, O. A., Bahamonde, J. R., Colmenero, J. R., Heredia, N., Villa, E., and Farias, P.: Emplacement of
738 the Cuera and Picos de Europa imbricate system at the core of the Iberian-Armorican arc (Cantabrian zone,
739 Nord Spain: New precisions concerning the timing of arc closure. *Geol. Soc. Am. Bull.* 121, 729-751, doi:
740 10.1130/B26366.1, 2009.
- 741 Merriman R. J. and Peacor D. R.: Very low-grade metapelites: mineralogy, microfabrics and measuring reaction
742 progress. In: M. Frey and D. Robinson (eds), *Low-Grade Metamorphism*, Blackwell Science, Oxford, 10-60,
743 1999.
- 744 Merriman, R. J. and Frey, M.: Patterns of very low-grade metamorphism in metapelitic rocks. In: Frey, M. and
745 Robinson, D. (eds), *Low grade metamorphism*, Blackwell Science, London, pp 61-107, 1999.
- 746 Meunier, A.: *Clays*, Springer-Verlag, Berlín, Heidelberg, New York, 2005.
- 747 Moore, D. M. and Reynolds, R. C. Jr. X-ray diffraction and the identification and analysis of clay minerals,
748 2nd ed., Oxford University Press, New York, 1997
- 749 Muchez, P., Heijlen, W., Banks, D., Blundell, D., Boni, M., and Grandia, F.: Extensional tectonics and the
750 timing and formation of basin-hosted deposits in Europe, *Ore Geol. Rev.* 27, 241-264,
751 doi:10.1016/j.oregeorev.2005.07.013, 2005.
- 752 Müllis, J.: The system methane-water as a geologic thermometer and barometer from the external parts of the
753 Central Alps, *B. Minéral.*, 102, 526-536, 1979.
- 754 Müllis, J., Rahn, M. K., De Capitani, C., Stern, W. B., and Frey, M.: How useful is illite “crystallinity” as a
755 geothermometer?, *Terra Nova*, 7, 128-129 (Supplement No. 1, Terra Abstracts), 1995.
- 756 Müllis, J., Rahn, M. K., Schwer, P., De Capitani, C., Stern, W. B., and Frey, M.: Correlation of fluid inclusion
757 temperatures with illite “crystallinity” data and clay minerals chemistry in sedimentary rocks from the
758 external parts of the Central Alps, *Schweiz. Mineral. Petrogr. Mitt.*, 82, 325-340, 2002.
- 759 Passchier, C. W. and Trouw, R. A. J.: *Microtectonics*, 2nd ed., Springer, Berlin, 366 pp, 2005.
- 760 Patrick, B. E., Evans, B. W., Dumoulin, J. A., and Harris, A. G.: A comparison of carbonate mineral and
761 conodont color alteration index thermometry, Seward Peninsula, Alaska, *Geological Society of America*,
762 *Abstracts with programs* 17, 399, 1985.
- 763 Phillips, G. N.: Widespread fluid infiltration during metamorphism of the Witwatersrand goldfields: generation
764 of chloritoid and pyrophyllite, *J. metamorph. Geol.*, 6, 311-332, 1988.
- 765 Raven, J. G. M. and van der Pluijm, B. A.: Metamorphic fluids and transtension in the Cantabrian Mountains of
766 northern Spain: an application of the conodont color alteration index, *Geol. Mag.*, 123, 673-681, 1986.
- 767 Rejebian, V. A., Harris, A. G., and Huebner, J. S.: Conodont color and textural alteration: an index to regional
768 metamorphism, contact metamorphism, and hydrothermal alteration, *Geol. Soc. Am. Bull.*, 99, 471-479,
769 1987.
- 770 Rodríguez Fernández, L. R.: La estratigrafía del Paleozoico y la estructura de la región de Fuentes Carrionas y
771 áreas adyacentes (Cordillera herciniana, NO de España), *Cuadernos do Laboratorio Xeolóxico de Laxe, Serie*
772 *Nova Terra*, 9, A Coruña, 240 pp. 1994.
- 773 Rodríguez Fernández, L. R. and Heredia, N.: La estratigrafía del Carbonífero y la estructura de la unidad del
774 Pisuerga-Carrión. NO de España, *Cuadernos do Laboratorio Xeolóxico de Laxe*, 12, 207-229, 1987.
- 775 Rodríguez Fernández, L. R., Heredia, N., Navarro, D., Martínez-García, E., and Marquínez, J.: Mapa Geológico
776 de España E. 1:50.000, Hoja N° 81, Potes. *Inst. Geol. Min. España*, 1994.

- 777 Savage, J. F.: Tectonic analysis of Lechada and Curavacas synclines, Yuso basin, León, NW Spain, *Leidse*.
778 *Geol. Med.*, 39, 193-247, 1967.
- 779 Środoń, J.: X-ray powder diffraction of illitic materials, *Clays Clay Miner.*, 32, 337-349, 1984.
- 780 Suárez, O. and Corretgé, L. G.: Plutonismo y metamorfismo en las zonas Cantábrica y Asturoccidental-leonesa,
781 in: Bea, F., Carnicero, A., Gonzalo, J. C., López Plaza, M., and Rodríguez Alonso, A. D. (eds) *Geología de*
782 *los granitoides y rocas asociadas del Macizo Hespérico (libro homenaje a L.C. García de Figuerola)*, Ed.
783 Rueda, Madrid, 13-25, 1987.
- 784 Suárez, O. and García, A.: Petrología de la granodiorita de Peña Prieta (León, Santander, Palencia), *Acta Geol.*
785 *Hispanica*, 9, 154-158, 1974.
- 786 Thompson, A. P.: A note on the kaolinite-pyrophyllite equilibrium. *Am. J. Sci.*, 268, 454-458, 1970.
- 787 Theye, T., Seidel, E., and Vidal, O.: Carpholite, sudoite, and chloritoid in low-grade high-pressure metapelites
788 from Crete and The Peloponnese, Greece, *Eur. J. Mineral.*, 4, 3, 487-507, 1992.
- 789 Valverde-Vaquero, P., Cuesta, A., Gallastegui, G., Suárez, O., Corretgé, L. G., and Dunning, G. R.: U-Pb dating
790 of late Variscan magmatism in the Cantabrian Zone (Northern Spain), Meeting of the European Union of
791 Geosciences 10 (EUG 10), Strasbourg, *Journal of Conference, Abstracts*, 4, 101, 1999.
- 792 Van der Pluijm., B. A., Savage, J. F., and Kaars-Sijpestijn, C. H.: Variation in fold geometry in the Yuso Basin,
793 northern Spain: implications for the deformation regime, *J. Struct. Geol.*, 8, 879-886, 1986.
- 794 Van Veen, J.: The tectonic and stratigraphic history of the Cardaño area, Cantabrian Mountains, Northwest
795 Spain, *Leidse. Geol. Med.*, 35, 45-104, 1965.
- 796 Velde, B.: *Introduction to clay minerals*, Chapman and Hall, 198 pp., 1992
- 797 Von Gosen, W., Buggisch, W., and Krumms, S.: Metamorphism and deformation mechanisms in the Sierras
798 Australes fold and thrust belt (Buenos Aires Province, Argentina). *Tectonophysics*, 185, 335-356
799 doi:10.1016/0040-1951(91)90453-Y, 1991.
- 800 Warr, L. N. and Rice, H. N.: Interlaboratory standardization and calibration of clay mineral crystallinity and
801 crystallite size data, *J. Metamorph. Geol.* 12, 141-152, 1994.
- 802 Winkler, H. G. F.: *Petrogenesis of metamorphic rocks*, 5th edition, Springer Verlag New York, 348 pp., 1979.
- 803 Zen, E-an: Metamorphism of Lower Paleozoic rocks in the vicinity of the Taconic Range in west-central
804 Vermont, *Am. Mineral.*, 45, 1-2, 129-175, 1960.
- 805

Variscan deformation	Emplacement of north-directed Palentine nappes (prior or earliest Moscovian) and the adjacent western Cantabrian nappes (late Moscovian) with associated thrusts in the PCU
Variscan deformation (cont.) (N-S shortening)	Emplacement of the south-directed Picos de Europa unit; thrusts and folds in the PCU (Kasimovian-Gzhelian) Upright folds and axial plane cleavage (S_1); first tectonothermal event with deep diagenetic – low anchizonal and ancaizonal areas in the northern part of the PCU (late Gzhelian)
Late Variscan gravitational readjustment; extensional event	Gently dipping cleavage (S_2) associated with crosscutting folds; second tectonothermal event; very low- or low-grade metamorphism (high anchizone-epizone, and ancaizone-epicaizone) in the syncline of Curavacas-Lechada and the VU. Normal faults (latest Gzhelian to early Cisuralian) Intrusion of igneous rocks, contact metamorphism and wide development of hydrothermal processes (Cisuralian)
Extension linked to the Basque-Cantabrian basin	Permian and Mesozoic hydrothermal episodes
Alpine deformation	N-S shortening, tightening of gentle folds, local crenulation cleavage and tilting of rocks northwards (Cenozoic).

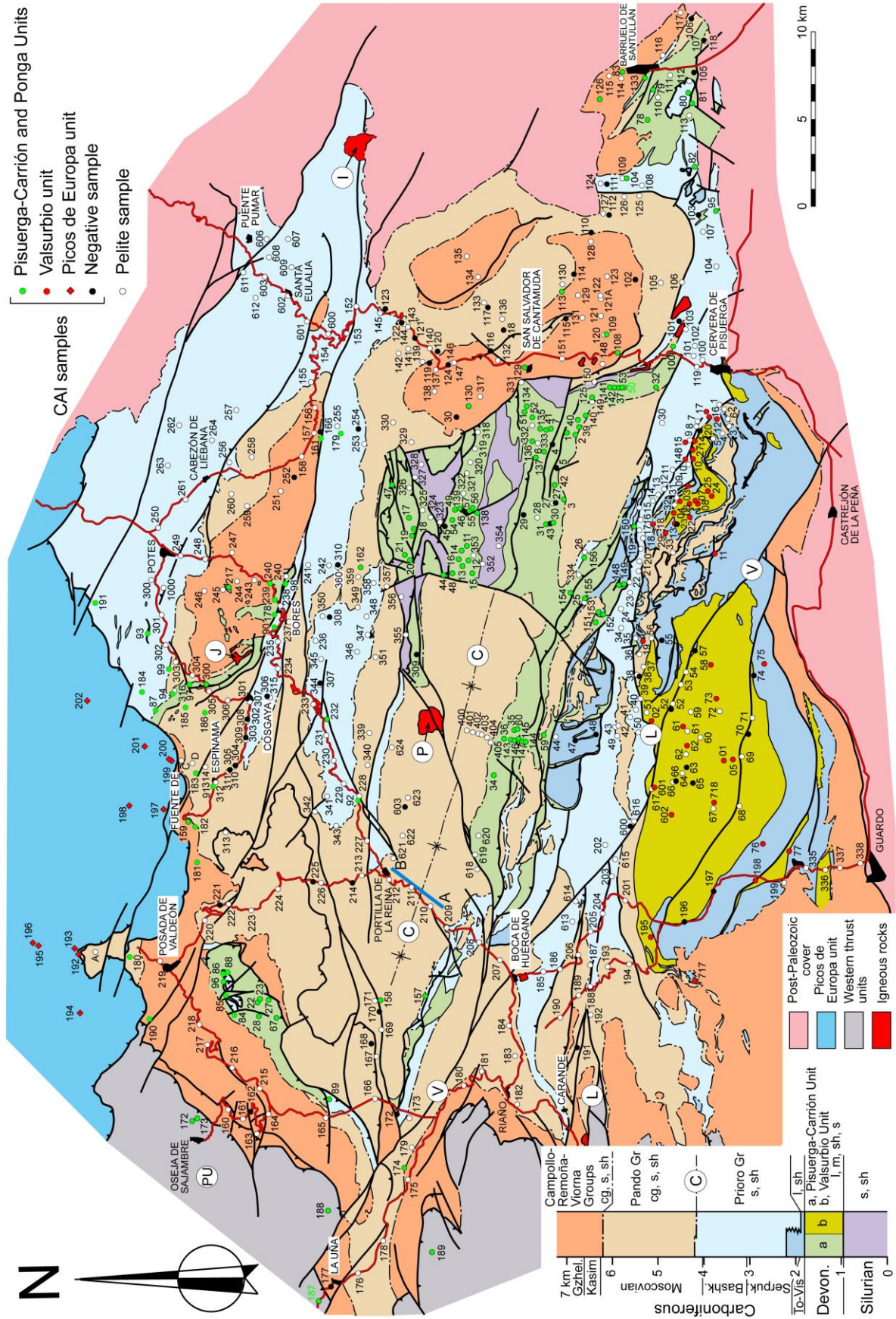
806 **Table 1. Tectonothermal evolution of the southeastern sector of the Cantabrian Zone.**



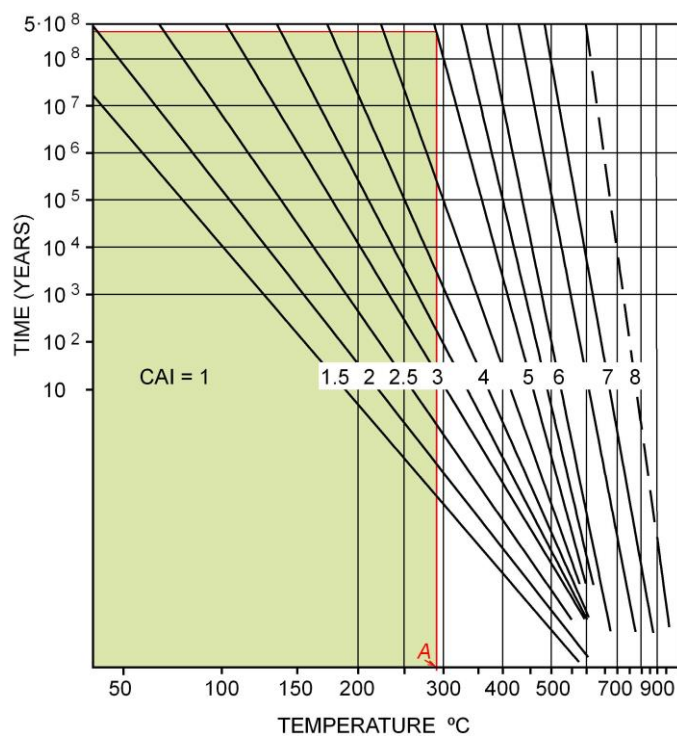
807

808 **Figure 1. Generalized geological map of the Cantabrian Zone (after Julivert 1971) showing major thrust**

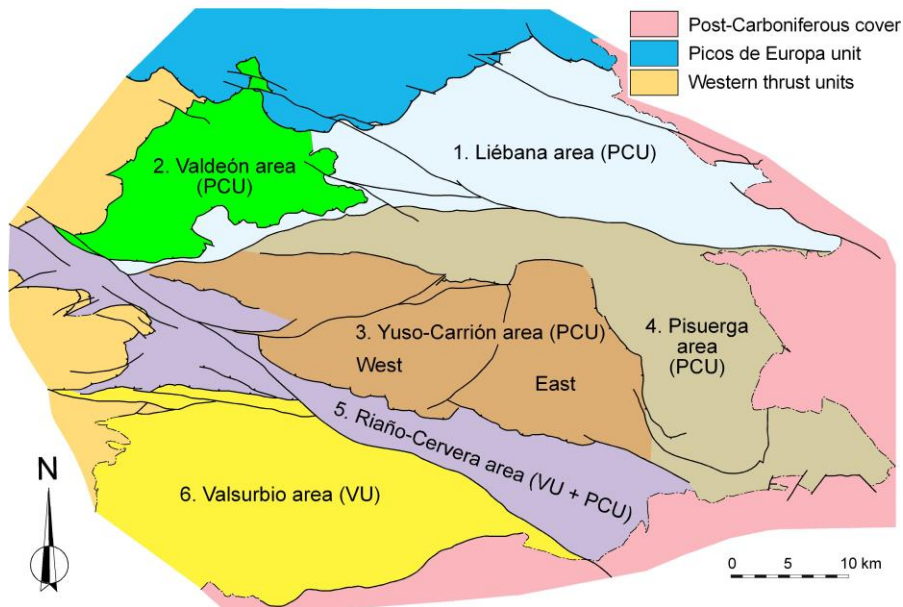
809 **units and the location of the study area.**



811 Figure 2. Geological map of the southeastern part of the Cantabrian Zone showing sampled localities
 812 (composed from Lobato, 1977; Colmenero et al., 1982; Ambrose et al., 1984; Julivert and Navarro, 1984;
 813 Martínez García et al., 1984; Lobato et al., 1985; Heredia et al., 1986, 1991, 1997; Rodríguez Fernández,
 814 1994; Rodríguez Fernández et al., 1994). Devonian and Silurian rocks of the PCU form the Palentine
 815 nappes. cg, conglomerate; l, limestone; m, marl; s, sandstone; sh, shale. C, Curavacas-Lechada syncline; I,
 816 Pico Iján granodiorite; J, Pico Jano granodiorite; L, León fault; P, Peña Prieta granodiorite; PU, Ponga
 817 unit; V, Ventaniella fault. Picos de Europa conodont samples after Bastida et al., 2004; Valsurbio
 818 conodont samples after García-López et al., 2013. A–B, location of cross-section in Fig. 11.

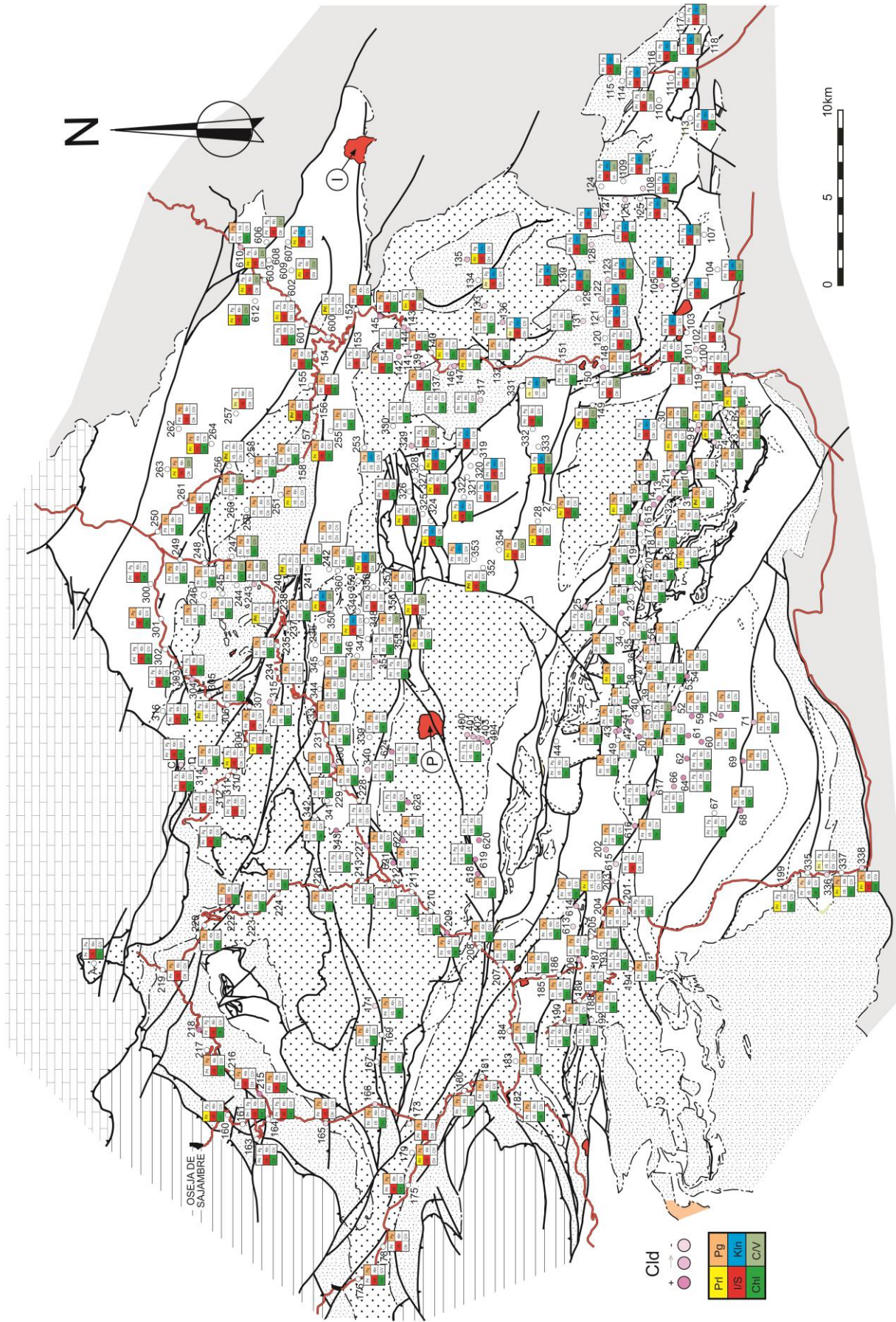


819
 820 Figure 3. Arrhenius plot to determine paleotemperature from CAI values (on the lines) and heating time
 821 (from Rejebian et al., 1987). Point A indicates the minimum temperature necessary to obtain a CAI = 5 for
 822 a rock with an age of 400 Ma. The green area shows the temperatures and heating times unable to
 823 produce CAI ≥ 5 in this rock.

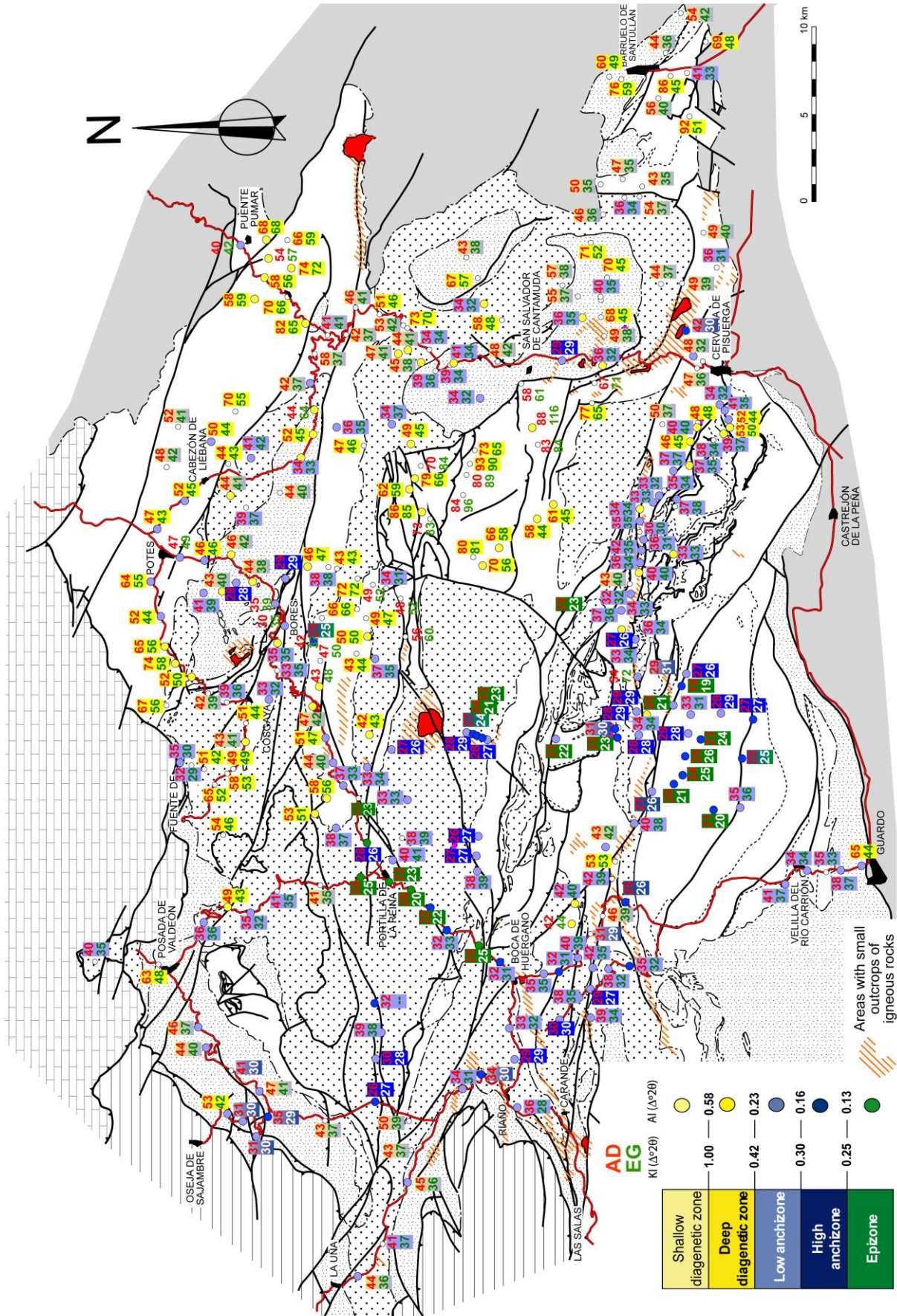


824

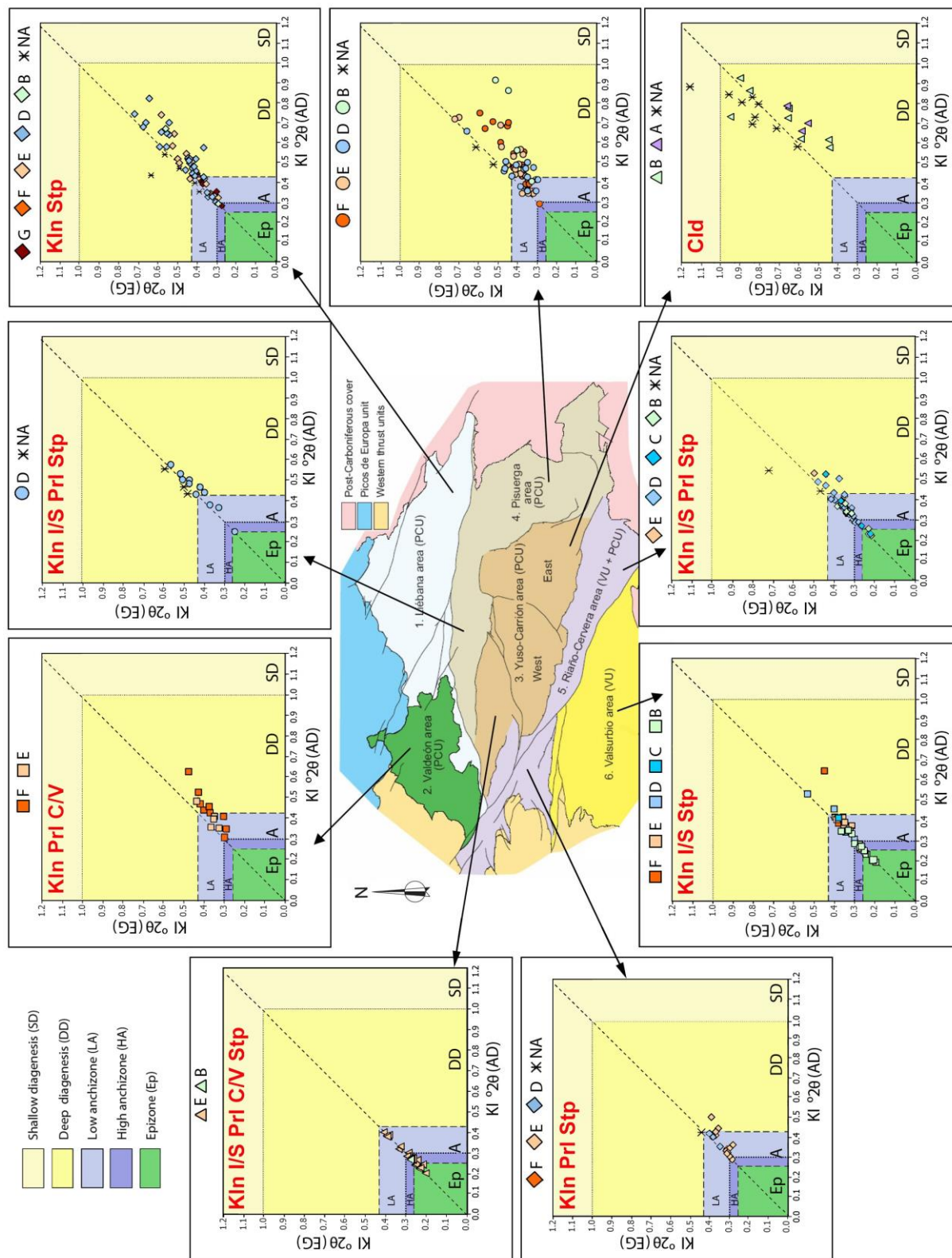
825 **Figure 4. Diagrammatic map indicating the areas in which the study units have been subdivided, following**826 **Martín-Merino et al. (2014)**



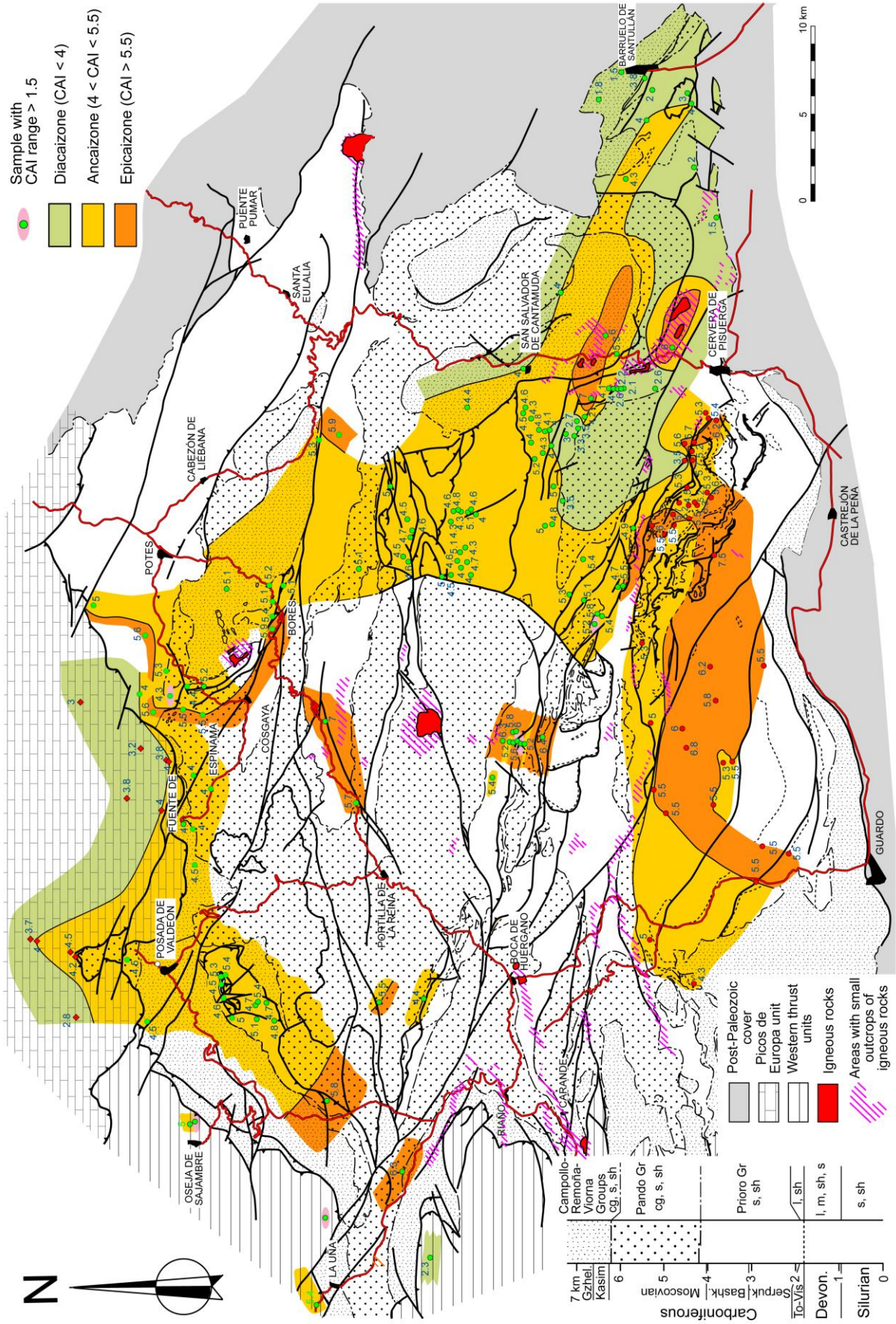
828 **Figure 5. Distribution of clay minerals in the study area. All the samples contain illite and therefore this**
829 **phase has not been considered in the plot. Presence of a certain phase in the sample is indicated by the**
830 **colour in the corresponding square. I, Pico Iján granodiorite; P, Peña Prieta granodiorite. For legend see**
831 **Figure 8.**



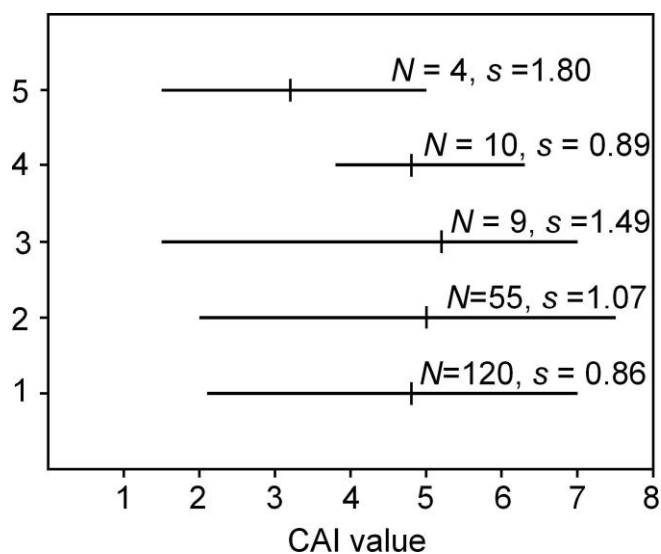
833 Figure 6. Map showing the location of Kübler Index (KI) values ($\times 100$) (Kübler scale). Upper value, in
 834 red, air dried sample; lower value, in green, sample treated with ethylene glycol. Árkai Index (AI) is
 835 indicated by the colour of the sampling point. Values corresponding to samples with significant amounts
 836 of I/S, PrI and/or Pg-Pg/Ms have not been highlighted with grade colours. For legend see Figure 8.



838 **Figure 7. Plot of Kübler Index (KI) measured on air dried (AD) versus KI measured on ethylene glycol**
839 **solvated samples (EG), standardized at Kübler scale. DD, Shallow Diagenesis; LA, Low Anchizone; HA,**
840 **High Anchizone; Ep, Epizone. Samples are plotted according to the areas outlined in Fig.4 and have been**
841 **grouped following the divisions of Fig. 2: A, Silurian; B, Devonian; C, Tournasian-Visean; D, Prioro**
842 **Group; E, Pando Group; F, Viorna Group; G, Campollo-Remoña Group. Samples with significant**
843 **amounts of I/S,Pr1 and/or Pg-Pg/Ms are indicated as NA (not applicable). Minerals absent in each of the**
844 **areas are indicated in red.**

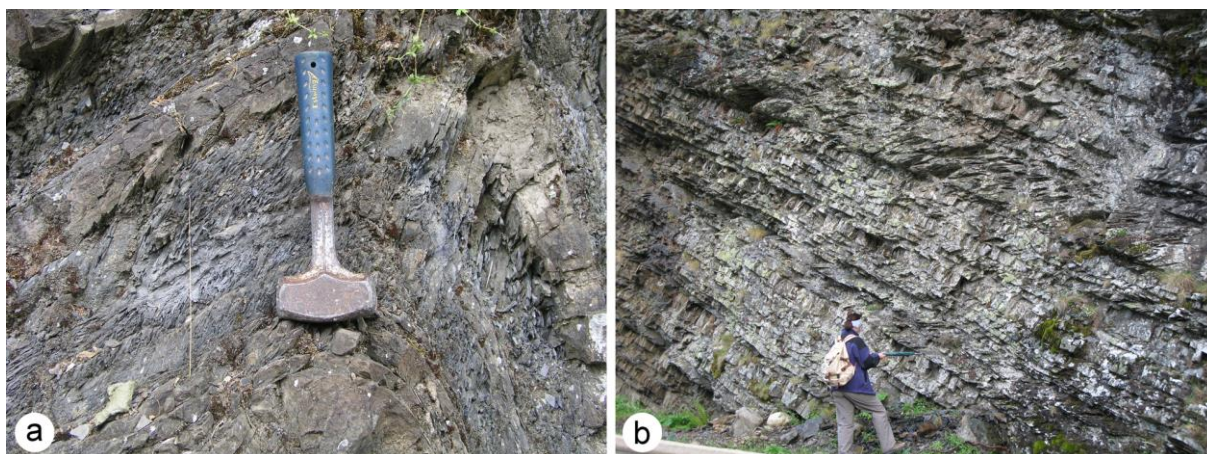


846 Figure 8. Map with location of CAI values and delimitation of CAI isogrades. Picos de Europa CAI data
 847 after Bastida et al., 2004; Valsurbio CAI data after García-López et al., 2013. Symbols of the CAI samples
 848 as in Fig. 2.



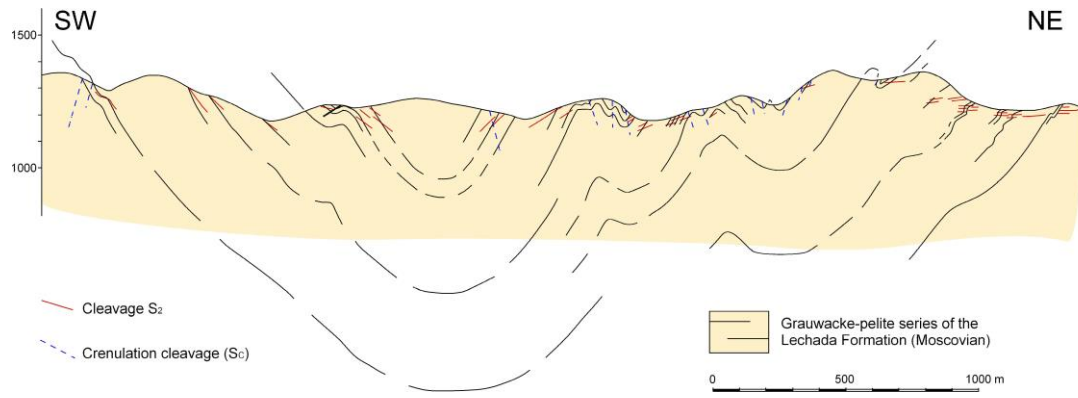
849

850 Figure 9. Diagram showing the distribution of CAI values in the different stratigraphic levels. The small
 851 vertical straight segments represent the mean value and the horizontal segments the CAI range. *N*,
 852 number of data; *s*, standard deviation. 1, Silurian-Devonian; 2, Tournaisian to lowermost Serpukhovian;
 853 3, lower Serpukhovian to lowermost Moscovian (Prioro Group); 4, lower-upper Moscovian (Pando
 854 Group); 5, Kasimovian-Gzhelian.



855

856 Figure 10. (a) S_1 cleavage associated with a nearly upright fold (eastern part of the Liébana area; north to
 857 the right). (b) S_2 cleavage **dipping less than bedding** in a normal stratigraphic succession (Pando Group;
 858 Curavacas-Lechada syncline; north to the left).



859

860 **Figure 11. Cross-section of the Curavacas-Lechada syncline showing the distribution of S_2 cleavage and**
 861 **crenulation cleavage. Location in Fig. 2.**

862 **Appendices (Supplement)**

863 **Appendix 1.** Conodont colour alteration index (CAI) values and temperatures inferred from the CAI Arrhenius
864 plot (Epstein et al., 1977; Rejebian et al., 1987). (V: Valsurbio samples; P: Pisuerga-Carrión samples; Po:
865 Ponga samples; Pe: Picos de Europa samples).

866 **Appendix 2.** Containing:

867 1. Values of Kübler Index (KI) measured on air dried (AD) *versus* KI measured on ethylene glycol solvated
868 samples (EG), standardized at Kübler scale. Samples are grouped according to the areas outlined in Fig. 4.
869 Samples with significant amounts of I/S and Pg-Pg/Ms that have not been plotted in Figs 6 and 7 are indicated
870 with Roman letter type of smaller size.

871 2. Árkai Index (AI) has been measured on air dried samples (AD).

872 3. Clay minerals present in the samples. Capitals and bold type indicate more abundance of the phase.

873

874

875

876